Nano-Micro Letters

ISSN 2311-6706
e-ISSN 2150-5551
CN 31-2103/TB

REVIEW

https://doi.org/10.1007/s40820-020-0404-8

Cite as
Nano-Micro Lett.
(2020) 12:70

Received: 24 December 2019
Accepted: 2 February 2020
Published online: 10 March 2020

Recent Advances of Persistent Luminescence Nanoparticles in Bioapplications

Shuqi Wu[1], Yang Li[1], Weihang Ding[1], Letong Xu[1], Yuan Ma[2], Lianbing Zhang[1] ✉

✉ Lianbing Zhang, lbzhang@nwpu.edu.cn

[1] School of Life Sciences, Key Laboratory of Space Bioscience and Biotechnology, Northwestern Polytechnical University, Xi'an 710072, People's Republic of China

[2] School of Materials Science and Engineering, Northwestern Polytechnical University, Xi'an 710072, People's Republic of China

HIGHLIGHTS

- Comprehensive summary on properties, persistent luminescence mechanism and synthesis of persistent luminescence nanoparticles.
- Unique properties and advantages of persistent luminescence nanoparticles for chem/biosensing, bioimaging and imaging-guided therapy.
- New organic and polymeric persistent luminescence nanoparticles with long afterglow lifetime for in vivo optical imaging.

ABSTRACT Persistent luminescence phosphors are a novel group of promising luminescent materials with afterglow properties after the stoppage of excitation. In the past decade, persistent luminescence nanoparticles (PLNPs) with intriguing optical properties have attracted a wide range of attention in various areas. Especially in recent years, the development and applications in biomedical fields have been widely explored. Owing to the efficient elimination of the autofluorescence interferences from biotissues and the ultra-long near-infrared afterglow emission, many researches have focused on the manipulation of PLNPs in biosensing, cell tracking, bioimaging and cancer therapy. These achievements stimulated the growing interest in designing new types of PLNPs with desired superior characteristics and multiple functions. In this review, we summarize the works on synthesis methods, bioapplications, biomembrane modification and biosafety of PLNPs and highlight the recent advances in biosensing, imaging and imaging-guided therapy. We further discuss the new types of PLNPs as a newly emerged class of functional biomaterials for multiple applications. Finally, the remaining problems and challenges are discussed with suggestions and prospects for potential future directions in the biomedical applications.

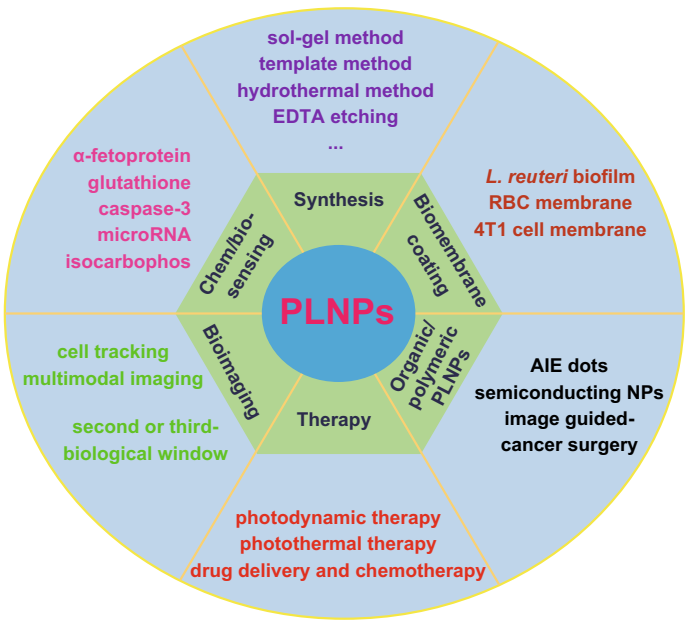

KEYWORDS Persistent luminescence nanoparticles; Biosensing; Bioimaging; Cell tracking; Cancer therapy

1 Introduction

Afterglow or persistent luminescence materials can store energy from UV light, visible light, X-ray or some other excitation sources and then gradually release it by a photonic emission [1–3]. The persistent emission can last for minutes, hours or even days after the stoppage of the excitation. The discovery of persistent luminescence phenomenon dates back to the Song Dynasty of China. Some paintings or so-called luminous pearls had incomprehensible magic to glow in the dark [4]. At the beginning of the seventeenth century, an Italian shoemaker first described the famous Bologna stone which emitted yellow to orange afterglow in darkness. Later, the natural impurities of BaS were found to play an important role in this persistent luminescence phenomenon. In 1996, Matsuzawa et al. reported a new phosphor of metallic oxide ($SrAl_2O_4$:Eu^{2+}, Dy^{3+}) which showed extremely bright and long phosphorescence [5]. Since then, persistent luminescence materials have been rapidly developed and lots of phosphors with different matrixes and doped ions have been reported. Up to now, inorganic metal compounds, metal–organic frameworks, some organic composites and polymers have been found to have long afterglow properties.

The unique properties of persistent luminescence materials mainly come from two kinds of active centers involved: the emitter centers and the trap centers [6–8]. The emitter centers can emit radiation after excitation. So, the emission wavelength of a persistent luminescence phosphor depends upon the emitter. The trap centers are formed due to impurities, lattice defects, or various co-dopants. They usually do not emit radiation, but store the excitation energy for some time and then gradually release it to the emitters by thermal or other physical activation. Therefore, the persistent intensity and time are mainly determined by the traps [2]. In design of persistent luminescence materials, a suitable emitter center and a proper host that can create appropriate traps and release long-lasting persistent luminescence (PL) should be considered [6].

There are persistent luminescence materials for each of the primary colors. Theoretically, we can synthesize persistent luminescence materials emitting any color by adjusting the chemical components. The most widely used and studied matrixes include silicates [9], gallium oxides [10], gallogermanates [11], aluminates [12] and so on [13–16]. Among them, $CaAl_2O_4$:Eu^{2+}, Nd^{3+} and $SrAl_2O_4$:Eu^{2+}, Dy^{3+} with overwhelming strong and long-lasting PL have been commercialized and widely used in various fields [2, 17]. With the fast development of persistent luminescence materials in recent years, some new phosphors with special compositions have been developed for multiple bioapplications, such as $Ca_3Ga_2Ge_3O_{12}$:Cr^{3+}, $Li_5Zn_8Al_5Ge_9O_{36}$:Cr^{3+} and $(Li, Na)_8Al_6Si_6O_{24}(Cl, S)_2$:$Ti^{3+}$ [18–20]. Tu et al. reported the rare-earth ions (Pr^{3+}, Nd^{3+} and Gd^{3+})-doped Li_2ZnGeO_4 with better afterglow properties due to their larger defect density values [21]. Furthermore, up-converting ions Yb^{3+}-Er^{3+}-incorporated $Zn_3Ga_2SnO_8$:Cr^{3+} showed an obvious near-infrared (NIR)-emitting PL after the stoppage of 980-nm laser irradiation [22]. These upconversion-persistent luminescence materials combined the advantages of both upconversion and persistent luminescence, paving a new way for biomedical applications [23–25].

Persistent luminescence materials emitting visible light have been successfully commercialized and widely used in security signs, traffic signs, dials, luminous paints and so on. In recent years, the deep-trap persistent luminescence materials with the unique characters of energy storage and controllable photon release showed great promising potential in the application of information storage, multilevel anti-counterfeiting and advanced displays [26–28]. Although the intensity and afterglow time of nanosized persistent luminescence nanoparticles (PLNPs) were much lower than the bulk materials [29, 30], PLNPs have been widely investigated as optical probes in bioimaging and biosensing due to the nanoeffects, the efficient cell penetration ability, the better biocompatibility, etc. [31]. Unlike conventional fluorescent probes (e.g., organic dyes, quantum dots, or upconversion nanoparticles) with very short lifetime, PLNPs can be used without constant in situ excitation. The persistent luminescence signals can be easily captured in the bioluminescence mode on imaging instruments. Furthermore, Cr^{3+}-doped PLNP with NIR emission open an extensive application in vivo, as the emission matches well with the first biological window (650–950 nm) and they can be re-activated with white or red LED light [3, 32–34]. The absence of autofluorescence background interferences and the NIR emission gave a high signal-to-noise ratio (SNR) and a better in vivo penetration depth. Through size and emission regulation, as well as surface modifications, PLNPs have been extensively used in biosensing, bioimaging and imaging-guided therapy as a new generation of advanced optical materials [35].

https://doi.org/10.1007/s40820-020-0404-8

Besides the most studied biosensing and bioimaging, scientists developed many novel PLNPs-based nanocomposites for special applications, such as antibacterium, latent fingerprint imaging and photocatalytic pollutant degradation [36–38]. In recent years, Nd^{3+}-doped PLNPs with the NIR emission located in the second (1000–1400 nm) or the third (1500–1800 nm) biological window have been developed to achieve high imaging depth and sensitivity [39, 40]. What is more, some organic PLNPs show promising advantages for in vivo afterglow imaging and detection [41, 42]. All these achievements make PLNPs novel multifunctional tools in bioapplications [43, 44]. A number of excellent reviews have already been published with the focus on the synthesis, surface engineering and biological applications of PLNPs. In 2017, Wang et al. summarized the recent achievements in biosensing, bioimaging and cancer therapy of PLNPs [45]. Sun et al. summarized their systematic achievements in the bioapplications of PLNPs from biosensing/bioimaging to theranostics. They developed target-induced formation or interruption of fluorescence resonance energy transfer (FRET) systems for biosensing and imaging of cancer biomarkers without autofluorescence interferences. They decorated targeting ligands or specific functional groups on PLNPs for tumor-targeted imaging, multimodal imaging and cancer therapy. They also proposed the design principle and comprehensive strategies for guiding and promoting further development of PLNPs in biological science and medicine [46]. Liang et al. summarized the design and applications of NIR-emitted PLNPs and emphasized their luminescence mechanism [47]. However, a review summarizing recent advances in synthesis methods, new types of organic/polymeric composition, biomembrane coating techniques, biosafety and bioapplications of PLNPs is lacking. The aim of this review is to present a comprehensive discussion on the synthesis and functionalization of PLNPs and the recent progress on PLNPs-based biosensing, bioimaging and therapy applications. This review further explores the future developments of PLNPs on the clinical applications (Scheme 1).

2 Typical Synthetic Procedures for PLNPs

In the past decade, various kinds of PLNPs have been synthesized by the solid-state synthetic methods with less control over the size and the shape of the products. As a result, the endured long reaction time and high annealing temperature of the synthesis make the phosphors bulky and irregular, which limit the usage in biomedical fields [34]. Therefore, new size- and shape-controllable synthetic methods have been developed to prepare nanosized PLNPs, such as sol–gel methods, template methods, hydrothermal/solvothermal methods and other wet-chemical synthesis methods [48–57]. In this section, we will discuss these typical synthetic approaches for PLNPs.

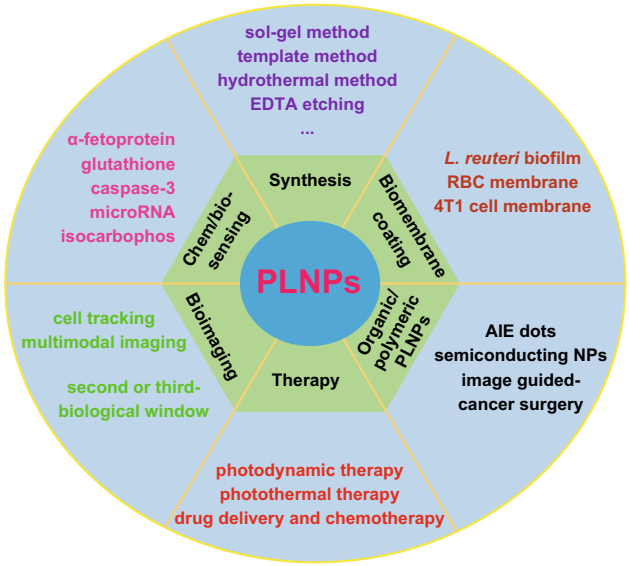

Scheme 1 Summary of advanced PLNPs for bioapplications

2.1 Sol–Gel Methods

Compared with the solid-state synthetic methods, the sol–gel methods can offer better purity, homogeneity and yield stoichiometric powders at relatively lower annealing temperature [58]. The synthetic conditions, including the reaction time, pH, temperature, concentration of the surfactants, chemical composition, etc., can be flexibly adjusted with the wet chemical synthesis. Abdukayum et al. reported the synthesis of NIR-emitting PLNPs by a citrate sol–gel method without the need for a reducing atmosphere. The authors assessed the effects of pH, annealing temperature, sinter time and composition on the luminescence intensity of PLNPs. It was found that the optimal pH of the starting solution is about 5. The increase in calcination time can promote the NIR persistent luminescence intensity at 1000 °C with the

proper composition of $Zn_{2.94}Ga_{1.96}Ge_2O_{10}:Cr_{0.01}Pr_{0.03}$ [33]. The resulting powder is usually in micrometer size scale, highly agglomerated and morphologically irregular. The main reason is due to the uncontrol over the nanoparticle growth stage and the agglomeration during the calcination with high temperature [59, 60]. Now, the wet grinding and selective sedimentation method have been used to isolate the smallest nanoparticles from the bulk materials, which suffers greatly from the trivial and time-consuming procedures with very low yield. The synthesized nanoparticles are usually non-spherical with a polydisperse size distribution in the range of 40–150 nm,which undoubtedly limits their advanced applications in biomedical fields.

2.2 Template Methods

Zhang and co-workers reported several works about the synthesis of PLNPs by a template method using mesoporous silica nanospheres (MSNs) [61–63]. MSNs can serve as both the morphology-controlling templates and the silicon source of some silicate PLNPs. The metal ions were impregnated in the mesopores of MSNs templates, followed by the annealing under certain conditions to form PLNPs with uniform morphologies and narrow size distributions. The template method can be easily transferred to synthesize PLNPs with different composition. The diameter and morphologies can be flexibly controlled by changing the MSNs templates [64]. However, up to now, MSNs was the only template that has been successfully used for synthesis of PLNPs. In addition, the high calcination temperature could destroy the surface functional groups, which may lead to the undesirable accumulation and poor dispersibility of PLNPs. As a result, the novelty and biomedical application of synthesizing functional PLNPs by template method are restricted.

2.3 Synthesis of Monodispersed PLNPs

The controlled synthesis of monodispersed and small sized PLNPs is essential for extended bioimaging and therapeutic applications, as large hydrodynamic-sized (> 100 nm) PLNPs are often quickly taken up and trapped in the reticuloendothelial system (RES). Therefore, it remains challenging to create nanosized PLNPs with high biocompatibility. The hydrothermal/solvothermal method, the non-aqueous sol–gel methods, the bi-phasic synthesis methods and other synthetic procedures are used to prepare monodispersed PLNPs [65–67].

In 2015, Li and co-workers first developed a direct aqueous-phase chemical synthesis route of NIR PLNPs (Fig. 1a). Their method leads to monodispersed PLNPs with the diameter as small as ca. 8 nm which present enhanced renewable NIR persistent luminescence in vivo. More importantly, such sub-10-nm PLNPs are readily functionalized and can be stably dispersed in aqueous solutions and cell culture medium for biological applications. Such nanocrystals possess superior red light renewable persistent luminescence both in vitro and in vivo, which can broad their use in photonics and biophotonics as advanced miniature "luminous pearls" [54]. Teston and co-workers designed a facile one-pot synthesis of ultra-small (6 nm) PLNPs by using a non-aqueous sol–gel method assisted with microwave irradiation (Fig. 1b). This strategy allows the control over the crystal growth by using the microwave heating as the energy source. The synthesized

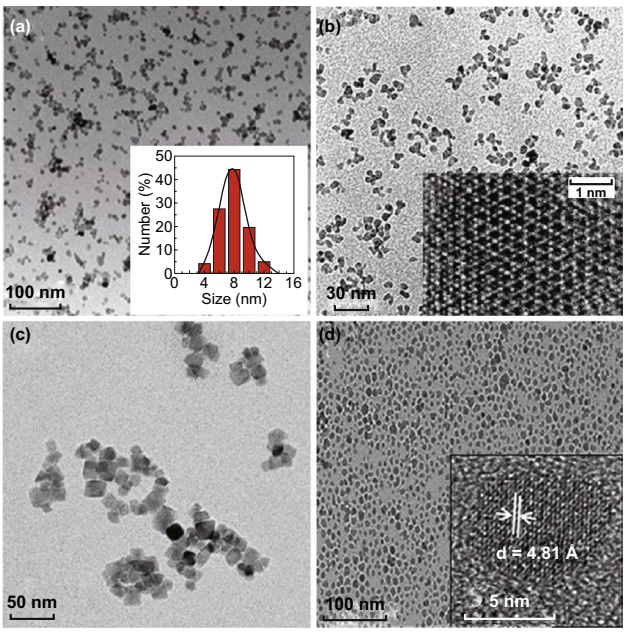

Fig. 1 The morphology of the monodispersed and small-sized PLNPs. **a** Direct aqueous-phase synthesis of sub-10-nm PLNPs. Reproduced with permission from Ref. [54]. Copyright 2015 American Chemical Society. **b** Synthesis of ultra-small PLNPs using a non-aqueous sol–gel method. Reproduced with permission from Ref. [50]. Copyright 2015 Wiley–VCH Verlag GmbH & Co. KGaA, Weinheim. **c** Silica shell-assisted synthetic route for synthesizing monodispersed PLNPs. Reproduced with permission from Ref. [67]. Copyright 2016 Tsinghua University Press and Springer-Verlag Berlin Heidelberg. **d** Synthesis of sub-10-nm PLNPs using a bi-phasic route. Reproduced with permission from Ref. [65]. Copyright 2012 The Royal Society of Chemistry

https://doi.org/10.1007/s40820-020-0404-8

PLNPs were then easily surface-modified with polyethylene glycol phosphonate moieties [50]. Recently, Zou et al. have established a robust and controllable three-step strategy involving the coating/etching of the SiO_2 shell to synthesize monodispersed PLNPs (~ 15 nm) without any agglomeration (Fig. 1c). This advanced strategy provides an ideal route to fabricate novel optical materials with excellent size distribution, dispersity and biocompatibility [67]. Srivastava et al. synthesized a sub-10-nm Cr-doped $ZnGa_2O_4$ nanoparticles by a bi-phasic synthesis route through the hydrolysis of inorganic salts in a water–toluene system (Fig. 1d). This synthesis strategy can control the particle size and shape by the slow nucleation process [65]. All these aforementioned methods provide feasible ways to synthesize monodispersed PLNPs and can be extended to synthesize other functional metal oxide nanoparticles.

In a similar fashion, Li and co-workers report the synthesis of 5-nm PLNPs with NIR emission at 800 nm via a direct aqueous-phase synthesis method [66]. This one-step hydrothermal synthetic route can easily produce PLNPs with abundant surface hydroxyl groups, avoiding complicated surface modification steps. Other synthesis routes using pulsed laser ablation, vacuum-annealing and surfactant-aided hydrothermal steps, etc., can provide ultra-bright monodispersed PLNPs with the super-long NIR persistent luminescence for in vivo bioapplications [68, 69]. For example, Wang et al. reported novel size-tunable hollow-structured PLNPs by crystallizing the immobilized parent ions on the carbon spheres and calcining. The large hollow cavity of PLNPs allows the high loading of chemical drugs and photosensitizers which can be used for chemo/photodynamic therapies (Fig. 2a) [70].

It is generally accepted that small size usually leads to short persistent luminescence and low quantum yield. To synthesize monodispersed small-sized PLNPs with bright and super-long afterglow remains challenging. Wang et al. reported the zinc gallogermanate PLNPs ($Zn_{1+x}Ga_{2-2x}Ge_xO_4$:Cr, $0 \le x \le 0.5$) with the composition-dependent size distribution and persistent luminescence. The intensity and decay time of the persistent luminescence can be fine-tuned by simply changing the formula [71]. Moreover, Wang and co-workers demonstrated

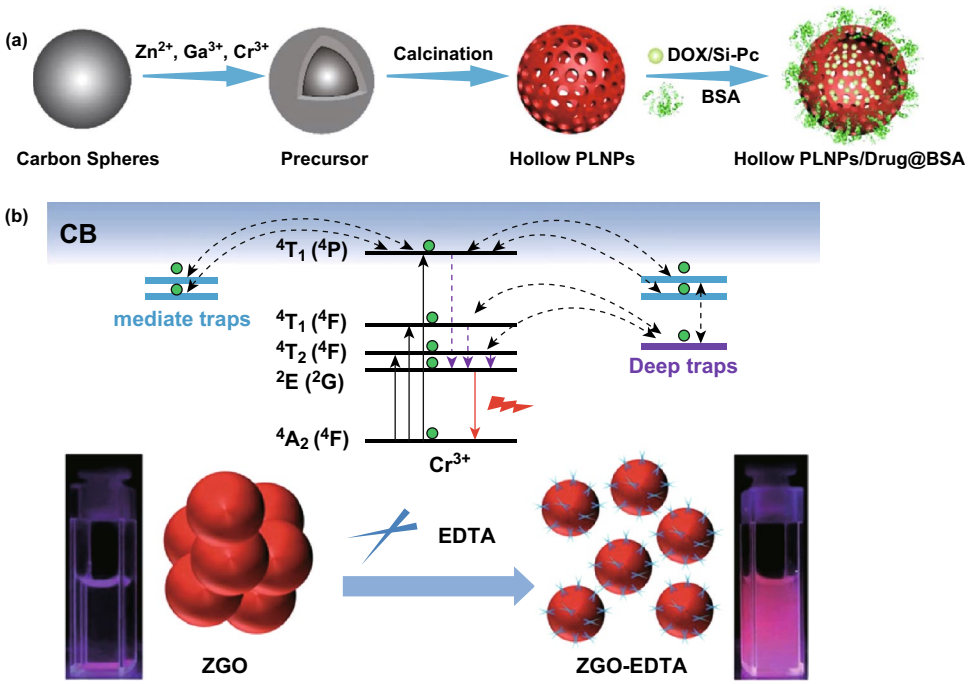

Fig. 2 **a** Synthesis and functionalization of the hollow NIR PLNPs. Reproduced with permission from Ref. [70]. Copyright 2018 American Chemical Society. **b** Regulating the traps, size and aqueous dispersibility of PLNPs by EDTA etching. Reproduced with permission from Ref. [72]. Copyright 2018 The Royal Society of Chemistry

a simultaneous control of the traps, size and aqueous dispersibility via a simple ethylenediaminetetraacetate (EDTA) etching. The resulting PLNPs-EDTA showed the suitable mediate/deep traps, a fine aqueous dispersibility and the super-long bright afterglows (Fig. 2b) [72]. The reported methods produced strong NIR-emitting and broadened the use of PLNPs in various research fields. Nonetheless, there are still many works needed to be done to deal with the tradeoff between the size and the persistent luminescence performance.

2.4 Biomembrane Bioinspired PLNPs

In order to avoid the recognition and phagocytosis by the immune system, multifunctional surface modification of nanodrug delivery systems was developed, including hydrophilic polymer modification, liposome encapsulation, tumor microenvironment responding strategies and so on. Li et al. reported the 4T1 tumor cell membrane-coated PLNPs-based nanocomposite for effective metastasis theranostic (Fig. 3a) [73]. This cancer cell membrane coating provided the

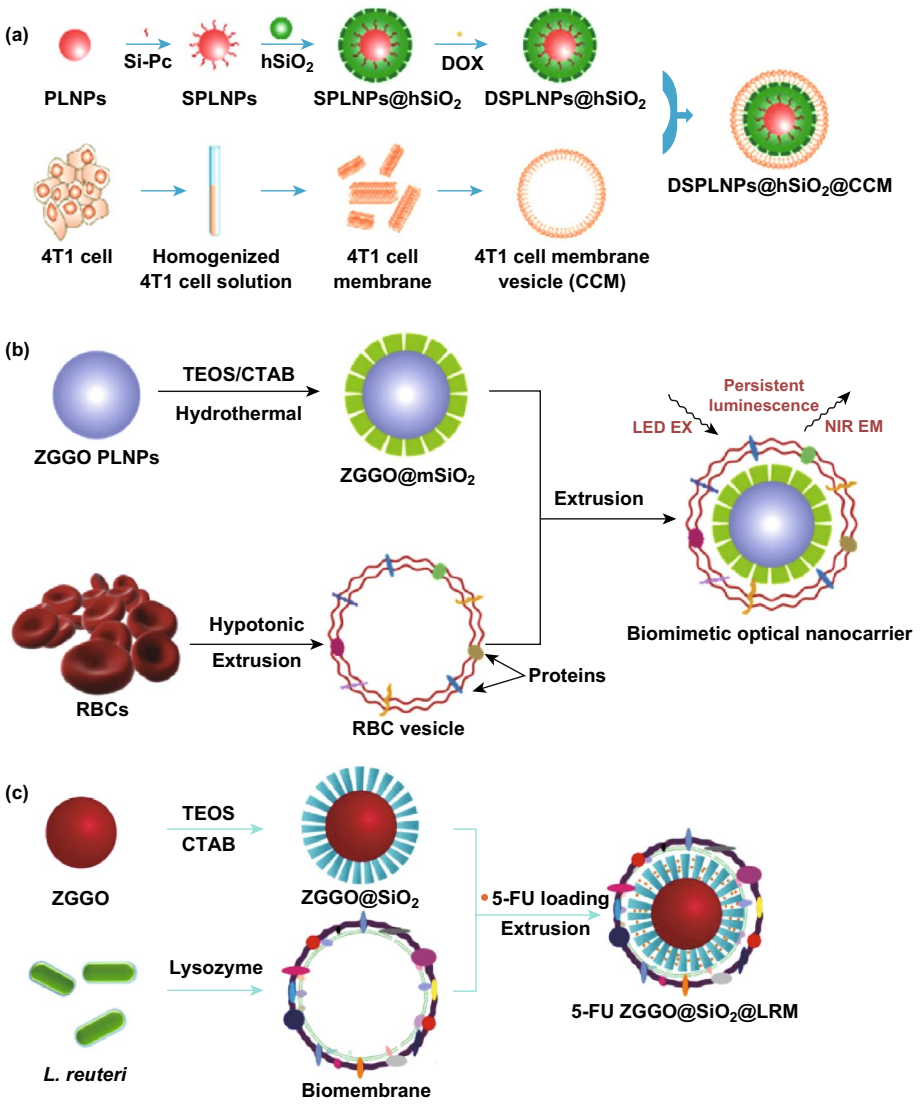

Fig. 3 **a** PLNPs nanocomposite was coated with 4T1 tumor cell membrane for PL imaging-guided chemo/photodynamic therapy of metastasis. Reproduced with permission from Ref. [73]. Copyright 2018 American Chemical Society. **b** PLNPs nanocomposite was coated with red blood cell membrane for in vivo long-circulating bioimaging and drug delivery. Reproduced with permission from Ref. [74]. Copyright 2018 Elsevier Ltd. **c** PLNPs nanocomposite was coated with *Lactobacillus reuteri* biofilm for colorectal cancer imaging and orally administrated chemotherapy. Reproduced with permission from Ref. [75]. Copyright 2019 American Chemical Society

 https://doi.org/10.1007/s40820-020-0404-8

nanocomposite with metastasis targeting ability and prevents the drug leakage. Due to the intrinsic biocompatibility and non-immunogenicity, red blood cell (RBC) membrane has also been successfully utilized to coat PLNPs-based nanocomposite as the biomimetic modifier (Fig. 3b) [74]. The RBC membrane-coated biomimetic nanocarriers showed a super-long persistent luminescence with the red-light renewability, a monodispersed nanosize and an excellent biocompatibility, which are suitable for in vivo long-circulating bioimaging and concomitant drug delivery. Moreover, *Lactobacillus reuteri* biofilm (LRM) was coated on the PLNPs nanocomposite for orally administered PL bioimaging and delivering colorectal cancer chemotherapeutic drug (Fig. 3c). This novel drug delivery system could protect the drugs from the gastric acid digestion and localize colorectum, which may give new prospects for oral drugs delivery [75]. These biomembrane-modified PLNPs nanoplatforms offer promising potential for targeted cancer imaging and therapy.

3 PLNPs for Chemo/Biosensing

High target selectivity and sensitivity of chem/biosensing probes play an important role in chem/biomedical detections. For example, the detection of tumor biomarkers, metabolites, biomolecules and other fundamental signal parameters in living cells is essential for disease theranostic and systematic studies on cell activities. Because of the elimination of the in situ excitation, PLNPs with long-lasting afterglow nature allow the chem/biosensing without background noise interferences. In particular, the NIR-emitting PLNPs showed the high penetration depth in biological tissues, the good photo- and chemical stability and the low toxicity which make them exceptionally favorable in chem/biosensing processes. PLNPs can be easily modified with various functional groups for the target detection and numerous efforts were devoted for chem/biosensing based on these functional PLNPs (Table 1) [76]. Among these works, the FRET pathways play a crucial role in the detection process. The following paragraphs will focus on several detection applications utilizing PLNPs.

The sensitive and selective sensing of biomarkers in biological environments is crucial for an efficient clinical diagnosis. Compared with the conventional fluorescent sensors based on dyes or QDs, PLNPs can provide noninvasive sensing both in vitro and in vivo and improve the detection limit by the elimination of the autofluorescence interferences. In 2011, Wu and co-workers established a FRET inhibition assay for α-fetoprotein (AFP) using water-soluble functionalized PLNPs ($Ca_{1.86}Mg_{0.14}ZnSi_2O_7$:$Dy^{3+}$, Eu^{2+}). The PLNPs were coated with polyethyleneimine and then conjugated with AFP antibody-coated gold nanoparticles. Au nanoparticles were served as the quencher due to their high molar adsorption coefficient. This highly sensitive and specific persistent photoluminescence probe can detect AFP in serum samples and real-time image the excreted AFP during the cancer cell growth (Fig. 4a) [77].

Similarly, Li and co-workers reported two works about PLNPs-based detection of GSH and ascorbic acid via FRET. PLNPs were used as the luminescence unit and the CoOOH nanoflakes or the MnO_2 nanoparticles as the quencher. The luminescence of PLNPs can be restored in the presence of ascorbic acid, as the CoOOH quencher was reduced to Co^{2+} [78]. For GSH detection, the presence of GSH reduced MnO_2 to Mn^{2+} which restored the luminescence [79]. These approaches provide effective platforms for detecting and imaging reactive species in living cells and tissues.

The aforementioned strategies use the nanoparticles as the persistent luminescence quenchers for "off–on" FRET detection. In addition, fluorescent dyes can also serve as luminescence quenchers or emit at different wavelength. Ju's group established three kinds of PLNPs-based nanoplatforms assembled by covalently binding fluorescent dye (FITC)-labeled peptides or DNA to carboxyl-modified PLNPs for the efficient detection of caspase-3 (Fig. 4b), microRNA and platelet-derived growth factor (PDGF) protein [80]. Wu et al. established a novel FRET immunoassay based on PLNPs for the prostate specific antigen (PSA) detection. The PLNPs conjugated with mouse monoclonal PSA antibody were employed as the energy donor, while Rhodamine B (RB)-bonded another PSA antibody was chosen as the energy accepter. PSA-mediated FRET from the modified PLNPs to RB resulted in the increase in the intensity ratio of RB (at 585 nm) to PLNPs (at 524 nm) with the increase in PSA concentration, which allow the efficient detection of PSA in serum and cell extracts (Fig. 4c) [81].

The impurities and other analytes in the complex samples may cause the high background noise and hamper the detection sensitivity and accuracy. For example, urine samples contain many kinds of small molecules, proteins and nucleic acids. Wang et al. published a PLNPs-based biochip with the

Table 1 Chem/biosensing based on functional PLNPs

Composition of PLNPs	Surface functionalization	Conjugation	Target	Detection mode	Limit of detection	Refs.
$Ca_{1.86}Mg_{0.14}ZnSi_2O_7:Dy^{3+}$, Eu^{2+}	PEI	Ab-AuNPs	α-Fetoprotein (AFP)	Off–on	0.41 μg L^{-1}	[77]
$Sr_2MgSi_2O_7:Eu^{3+}$, Dy^{3+}	Hydroxylated	CoOOH nanoflakes	Ascorbic acid	Off–on	2.20 μM	[78]
$Sr_2MgSi_2O_7:Eu^{3+}$, Dy^{3+}	Hydroxylated	MnO_2 nanosheets	Glutathione	Off–on	0.83 μM	[79]
$Sr_{1.6}Mg_{0.3}Zn_{1.1}Si_2O_7:Eu^{2+}$, Dy^{3+}	FITC-labeled substrate peptide	–	Caspase-3	On–off	2.4×10^5 unit mL^{-1}	[80]
$Sr_{1.6}Mg_{0.3}Zn_{1.1}Si_2O_7:Eu^{2+}$, Dy^{3+}	FITC-labeled DNA	–	MicroRNA-21	Off–on	0.26 pM	[80]
$Sr_{1.6}Mg_{0.3}Zn_{1.1}Si_2O_7:Eu^{2+}$, Dy^{3+}	FITC-labeled aptamer	–	Platelet-derived growth factor (PDGF)	On–on	2.57 pM	[80]
$Ca_{1.86}Mg_{0.14}ZnSi_2O_7:Dy^{3+}$, Eu^{2+}	PSA antibody	Rhodamine B-bonded PSA antibody	Prostate specific antigen (PSA)	On–on	0.09 μg L^{-1}	[81]
$SrMgSi_2O_6:Eu^{3+}$, Dy^{3+}	–	–	Dopamine	On–off	0.78 μM	[83]
$Zn_2GeO_4:Mn^{2+}$	Lysozyme-binding aptamer	Black-hole-quencher-labeled DNA (BHQ-DNA)	Lysozyme	Off–on	4.6 nM	[166]
$Zn_2GeO_4:Mn$	–	Gold nanoparticles–aptamer complex	Isocarbophos	On–off	7.1 μg L^{-1}	[167]
$Cr^{3+}_{0.004}:ZnGa_2O_4$	Au nanoparticles	Cy5.5-KGPNQC-SH	Fibroblast activation protein-alpha (FAPα)	Off–on	115 pM	[168]
$Zn_{1.25}Ga_{1.5}Ge_{0.25}O_4$:0.5%$Cr^{3+}$	LTA antibody	–	Foodborne probiotics	On–on	–	[84]
$ZnGa_2O_4:Cr^{3+}$	Insulin-binding aptamer	Au complex	Insulin	Off–on	2.06 pM	[169]
$ZnGa_2O_4:Cr^{3+}$	–	–	Hemoglobin	On–off	0.13 nM	[170]
$Sr_2Al_{14}O_{25}:Eu^{2+}$, Dy^{3+}	–	–	antibiotics	On–off	5 nM	[171]
$Sr_2Al_{14}O_{25}:Eu^{2+}$, Dy^{3+}	–	–	2,4,6-Trinitrophenol	On–off	10 nM	[171]
$Zn_2GeO_4:Mn$	Single-stranded DNAs	Black-hole-quencher-labeled DNAs	Bladder cancer-related miRNA	Off–on	26.3 fM	[82]
$ZnGa_2O_4:Cr^{3+}$	Polyethyleneimine	Dithiothreitol-coated gold nanorods	Arsenic(III)	Off–on	55 nM	[172]

enhanced persistent luminescence signals and the ultra-low autofluorescence background interferences for bladder cancer-related miRNA-21 detection in urine (Fig. 5). Using the time-gated luminescence of PLNPs, the detection sensitivity was significantly improved and a detection limit of 26.3 fM was achieved [82]. This sensitive PLNPs-based detection of the disease-related biomarkers in patient urines can open up a new avenue in painless and noninvasive diagnosis.

The PLNPs-based nanoplatform was employed to detect other important parameters and biomolecules, such as dopamine, temperature, avidin and foodborne probiotics [83–86]. Furthermore, PLNPs-based detection can be produced as the assay reporters in the lateral flow assays [87]. The sensitive and selective detection without background interferences in complex biological samples is urgently needed for medical diagnosis, therapy monitoring and health management. For instance, the detection of heavy metal ions (Hg^{2+}, Pb^{2+}, etc.), reactive oxygen species (ROS) and high toxic molecules plays an important role in life sciences. Although biosensing based on PLNPs has been reported in many publications, more efforts need to be done before the clinical use.

https://doi.org/10.1007/s40820-020-0404-8

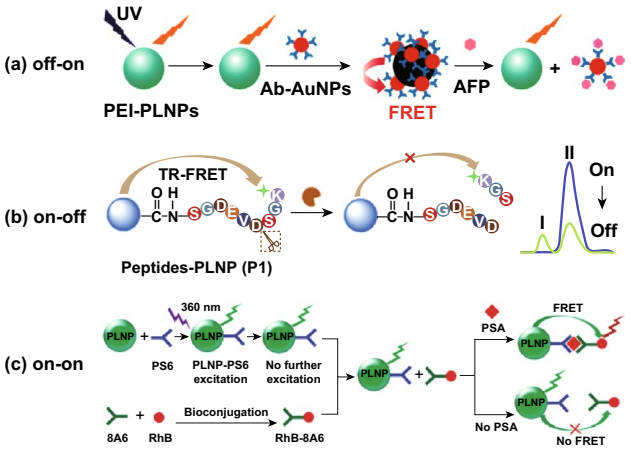

Fig. 4 Schematic illustration of PLNPs-based biosensing. **a** FRET inhibition assay for AFP based on the PL quenching of PEI-PLNPs by antibody (Ab)-AuNPs. Reproduced with permission from Ref. [77]. Copyright 2010 American Chemical Society. **b** Detection strategies of caspase-3 protease by using caspase-specific peptide-functionalized PLNPs probe. Reproduced with permission from Ref. [80]. Copyright 2015 Elsevier Ltd. **c** Design for PSA detection using PLNPs-based FRET immunoassay. Reproduced with permission from Ref. [81]. Copyright 2015 The Royal Society of Chemistry

4 PLNPs for Bioimaging

PLNPs were first used by Scherman and co-workers for in vivo imaging [88]. PLNPs without the continuous in situ excitation can efficiently eliminate the background autofluorescence from animal tissues in bioimaging, leading to the significant improvement of the imaging sensitivity and the signal-to-noise ratio (SNR). With the large surface-to-volume ratio, surface modifications can be easily achieved by silica coating, polymer linking, biomolecules conjugation and so forth, after which PLNPs are ready to be employed into extensive bioimaging applications. Compared to conventional in vivo optical imaging probes, PLNPs possess high photostability, superior SNR and excellent biocompatibility and can be directly used in the commercially available imaging systems. Importantly, the long afterglow and red-light renewable capability permit PLNPs to be used for long-term in vivo bioimaging applications [44, 89, 90].

4.1 Cellular Imaging and Tracking

PL imaging allows noninvasive tracking and imaging for visualizing various biological processes of migrating cells, which might be crucial for the biological fate and progression of some diseases. Up to now, imaging of Raw 264.7 macrophages (a phagocytic cell line), stem cells, breast cancer cells, J774A.1 macrophages have been widely studied by labeling with PLNPs [91–95]. Maldiney et al. and Chuang et al. reported the noninvasive long-term in vivo tracking of RAW 264.7 cells with PLNPs. The RAW cells can be efficiently labeled with PLNPs by simple incubation. As the NIR-emitting light has the better penetration, PLNPs labeling can track RAW cells during cell homing process in vivo [3].

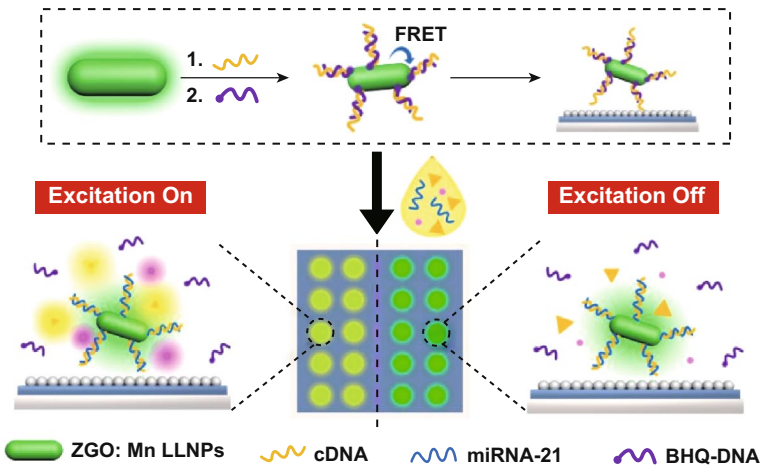

Fig. 5 Time-gated detection of bladder cancer-related miRNA-21 by the developed PLNPs-based biochip. Reproduced with permission from Ref. [82]. Copyright 2019 American Chemical Society

We established the first fabrication of TAT penetrating peptide-functionalized PLNPs for the long-term tracking of adipose-derived stem cells (ASC). We used the skin-regeneration and tumor-homing models to study the in vivo tracking and imaging efficiency. PLNPs showed very promising results for ASC tracking without affecting the natural behavior of ASC, which provides us insights to study the fate and migration of ASC [35]. Early detection of cancer metastasis is quite essential and challenging for the cancer diagnosis and treatment. The outstanding advantages of PLNPs in cell imaging show great potential for tracking cancer cell metastasis. Liu et al. reported the PLNPs-based real-time tracking of the orthotopic breast cancer cell metastasis, and its guidance for surgical resection (Fig. 6) [96]. Zhao et al. prepared PLNPs containing a hydrogel (PL-gel) for targeted, sustained and autofluorescence-free tumor metastasis imaging (MBA-MD-231 breast cancer cells). This PL-gel could be rationally designed to target variety of other cancer cells and provide a powerful and versatile method for studying tumor metastasis [97].

PLNPs-based labeling strategies also have universal applications in monitoring other cancer cells. For example, Maldiney et al. reported the first use of biotinylated PLNPs to target the avidin-expressing glioma cells, which provided preliminary results for guiding the use of avidin–biotin technology to target the glioma tumor microenvironment [69]. Zhao et al. conjugated two targeting ligands (hyaluronic acid and folic acid) on the PLNPs, which target specifically toward the cluster determinant 44 receptor and the folic acid receptor on the tumor cells. This dual-targeting strategy provides synergistic effects to improve the specificity and affinity toward the cancer cells [98]. These cellular target imaging and tracking approaches not only inspire studies on the fate of cells in important life activities but also broaden the applications in cell-based research and therapy.

4.2 In Vivo Multimodal Imaging

To date, various imaging techniques have been developed for monitoring various biological processes and visualizing pathogenesis and progression of many diseases, such as the X-ray computed tomography imaging (CT), the magnetic resonance imaging (MRI) and the optical imaging. The PLNPs-based PL imaging (PLI) shows high SNR, easy operation and deep penetrating depth capabilities. Thus, the integration of the PL imaging with other imaging techniques can bridge the gaps in resolution, sensitivity and depth [43]. Several groups have introduced the engineering of multifunctional platforms based on PLNPs for the multimodal imaging (Table 2). The combination of PLI and MRI is most frequently studied [99–103]. These promising nanoprobes as novel diagnosis techniques will open wide applications for biologists and pharmacologists in biomedical research [104–106].

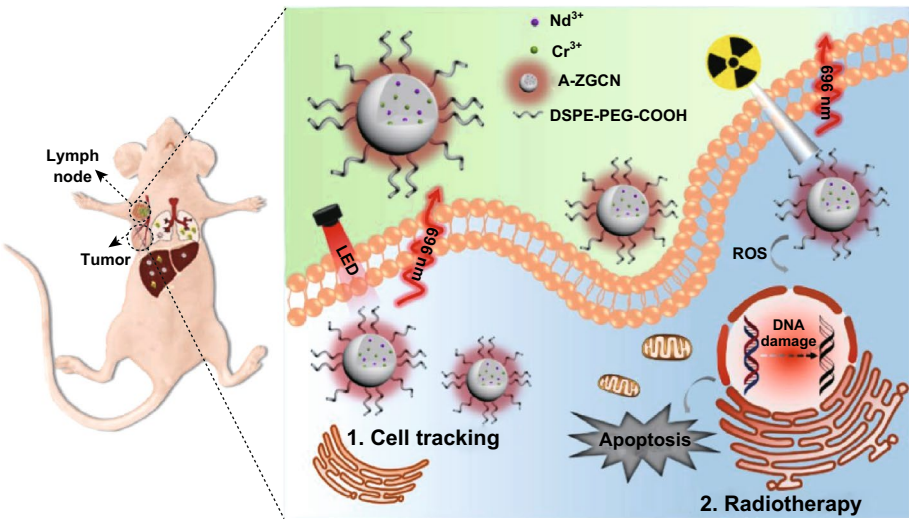

Fig. 6 In vivo tracking of breast cancer cells and inhibiting tumor metastasis by radiotherapy with engineered A-ZGCN nanoparticles. Reproduced with permission from Ref. [96]. Copyright 2019 American Chemical Society

 https://doi.org/10.1007/s40820-020-0404-8

Table 2 Typical multimodal in vivo imaging studies with PLNPs

Imaging modalities	Composition of PLNPs	Surface modification	Biological model	Refs.
PL/MRI	$Zn_{2.94}Ga_{1.96}Ge_2O_{10}:Cr^{3+}$, Pr^{3+}	Gd-DTPA	Biodistribution	[99]
PL/MRI	Gd-doped $ZGaO:Cr^{3+}$	PEG	Biodistribution	[43]
PL/MRI	$Gd_2O_3@mSiO_2@CaTiO_3:Pr^{3+}$	PEG	Biodistribution	[101]
PL/MRI	$ZGaO:Cr^{3+}@$ $mSiO_2$-USPIOs	Diglycolic anhydride	Biodistribution	[102]
PL/MRI	Gd_2O_3-$ZnGa_2O_4:Cr^{3+}$	Hyaluronic acid (HA)	Tumor imaging	[103]
PL/CT	$Zn_{2.94}Ga_{1.96}Ge_2O_{10}:Cr^{3+}$, $Pr^{3+}@TaO_x@SiO_2$	Cyclic-Asn-Gly-Arg peptides	Tumor imaging	[104]
PL/MRI/CT	$GdAlO_3:Mn^{4+}$, $Ge^{4+}@SiO_2@Au$	–	Tumor imaging	[106]

The in vivo multimodal imaging studies are mostly performed on mice. Maldiney and co-workers introduced the first synthesis and functionalization of a multimodal PLI/MRI nanoprobe based on the gadolinium-doped PLNPs. This novel imaging probe combines the high sensitivity from the PLI with the high spatial resolution of the MRI. The CT serves as a conventional medical imaging technique for a period of time, due to its promising features in high spatial resolution and ease of illustrating 3D biological structures. Lu et al. reported the fabrication of TaO_x and PLNPs for a PL/CT bimodal imaging. This multifunctional nanoparticle could act as a new potential platform for the tumor imaging with high SNR, low toxicity and good spatial resolution [104]. Liu and co-workers reported $GdAlO_3:Mn^{4+}$, $Ge^{4+}@Au$ (GAMG@Au) core–shell nanoprobes for in vivo tri-modality (PLI/MRI/CT) bioimaging (Fig. 7). The NIR persistent luminescence and the doped Gd element were used for the optical imaging and the magnetic resonance imaging, respectively. The gold nanoshell coated on the PLNPs could not only serve as the CT imaging agent but also enhance the PL efficiency via the plasmon resonance [106].

PLNPs-based optical bioimaging agents have been used in some subcutaneous-tumor bearing mouse models for tumor imaging or biodistribution study. In addition, PLNPs-based nanocomposites could be applied in other important biological models [107]. For example, in the lymphatic imaging, PLNPs could be potentially applied to monitor the location of lymph nodes and study the lymph node functions [108]. We believe that PLNPs are ideal for the long-term monitoring of the considerable biological processes in real time, including the imaging on bacteria, *C. elegans* or zebrafish models in the future.

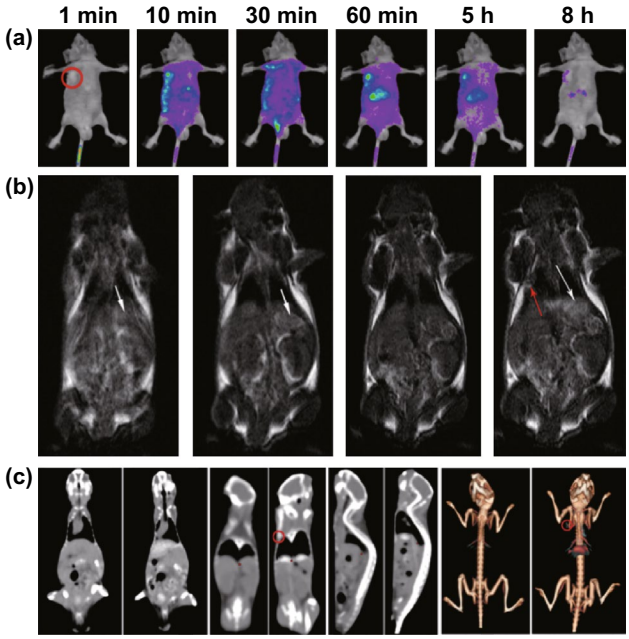

Fig. 7 In vivo trimodal bioimaging. **a** PL images at different time points. **b** T_1-weighted MRI coronal images. **c** CT coronal view images. Reproduced with permission from Ref. [106]. Copyright 2016 American Chemical Society

4.3 X-ray Irradiated PLNPs for In Vivo Imaging

Currently, the NIR-emitting PLNPs are mainly excited by UV, visible light or red LED light. The relatively short penetration depth of these lights hindered the application for deep tissue imaging. In fact, PLNPs can also be excited by X-ray [109–112]. The development of soft X-ray excitation source with low power in recent years broadens the applications of PLNPs, as it can restore in vivo imaging signals even at 20 mm depth. The NIR-emitting $ZnGa_2O_4$:Cr PLNPs can be repeatedly activated with low-power X-ray. After the intravenous injection or the oral administration, the in vivo whole-body bioimaging was successfully achieved under X-ray

irradiation (Fig. 8). Compared to the traditional UV and visible excitation sources, X-ray shows competitive advantages of deeper penetration depth and weaker scattering in tissues which activates PLNPs to emit NIR persistent luminescence for in vivo deeper tissue bioimaging [113–115].

4.4 In Vivo PL Imaging in the Second or Third Biological Window

It is well accepted that NIR emission can penetrate biological tissues, such as skin, blood and organs, more efficiently than visible light. However, the light in the second (1000–1400 nm) and the third (1500–1800 nm) NIR biological windows shows the lower absorption, the lower scattering coefficient and the deeper tissue penetration than the light in the first NIR window (650–950 nm). Nie et al. reported new Ni-doped PLNPs with a tunable emission band peaking from 1270 to 1430 nm in the second NIR window (Fig. 9a). These long NIR emitting PLNPs with characteristic operational waveband and excellent tunability offer the possibility for visualizing structural and functional process in cells, tissues and other complex systems [40]. Cr^{3+}/Er^{3+}-co-doped $LaAlO_3$ perovskite phosphors exhibit two long PL bands at 734 (first window) and 1553 (third window) nm (Fig. 9b). These NIR-emitting PLNPs lead to an improved contrast quality and deeper tissue penetration depth than the Cr^{3+}-doped PLNPs with the emission in the first NIR window [116–119].

5 PLNPs-Based Imaging-Guided Therapy

In recent years, PLNPs have been positively involved in theranostic studies, as the persistent luminescence can be used to determine the accurate position and time that therapy required, alleged "imaging-guided therapy." Among various therapeutic technologies, chemotherapy, photodynamic therapy (PDT) and photothermal therapy (PTT) are mostly studied due to their obvious treatment effects. With the

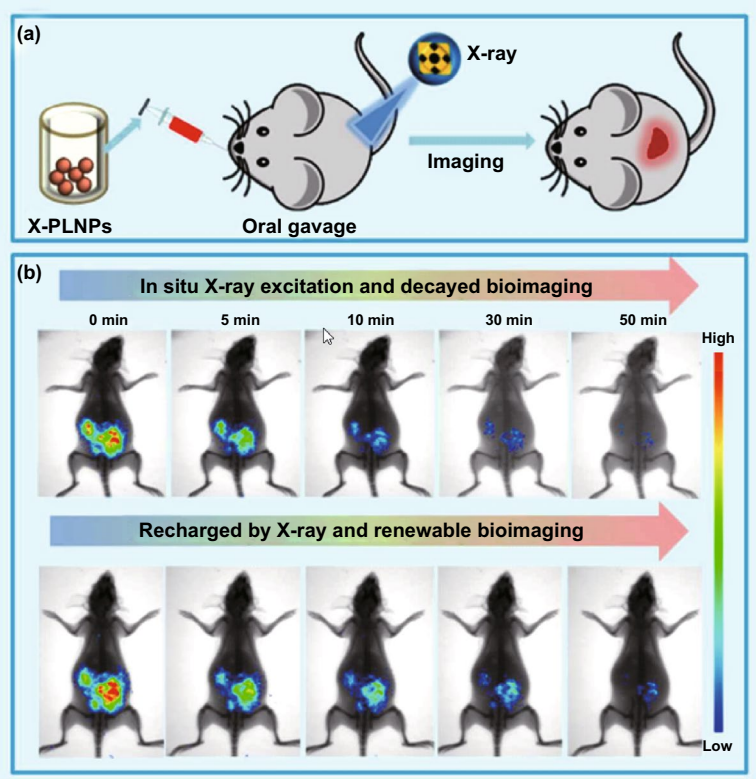

Fig. 8 **a** In vivo bioimaging after the oral administration of PEG-modified PLNPs under X-ray irradiation. **b** Rechargeable in vivo whole-body imaging of mouse with oral administrated PLNPs at different time after stoppage of X-ray excitation. Reproduced with permission from Ref. [114]. Copyright 2017 The Royal Society of Chemistry

https://doi.org/10.1007/s40820-020-0404-8

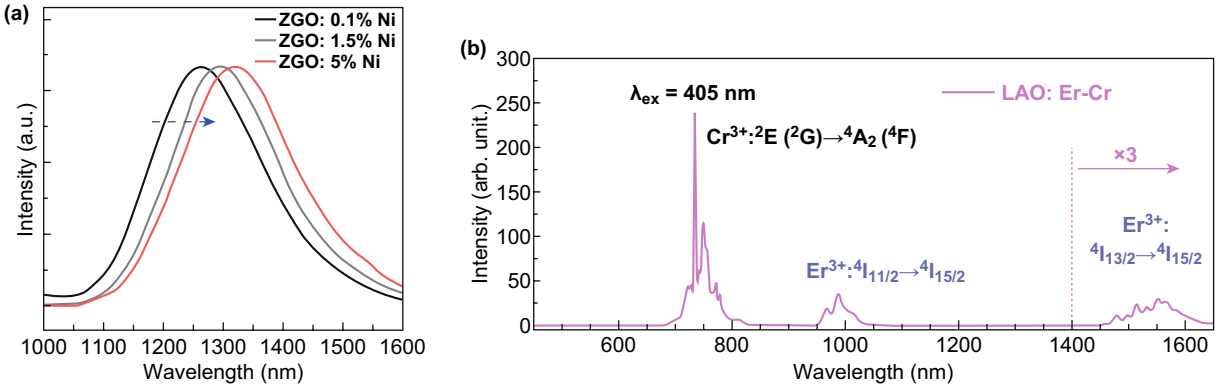

Fig. 9 In vivo PL imaging in the second or third biological window. **a** PL spectra in the second imaging window. Reproduced with permission from Ref. [40]. Copyright 2017 Springer Nature. **b** PL spectra in the first and third imaging windows. Reproduced with permission from Ref. [117]. Copyright 2017 The Royal Society of Chemistry

remarkable penetration depth and biocompatibility, PLNPs can be integrated to provide various PL imaging-guided therapies [120].

5.1 PLNPs-Based Drug Delivery and Chemotherapy

Chemotherapy is one of the most used cancer therapies, although its disadvantages of the drug resistance and the side effects or toxicity on healthy tissues limit the clinical effectiveness. Many nanoparticle-based drug delivery systems have been developed for simultaneous imaging and chemotherapy, which realizes the real-time monitoring of the treatment, the photo-controllable targeting and less side effects. Usually, mesoporous or hollow silica nanoparticles are integrated on the PLNPs as trackable drug carriers due to their large pore structure and specific surface areas [63, 121]. These platforms with high drug storage capacity and excellent NIR persistent luminescence show promising potential for the delivery of any therapeutic agents as the trackable drug carriers.

Chen and co-workers established liposome-encapsulated PLNPs as novel PL imaging-guided drug carriers for chemotherapy. Since liposomes have been extensively used as drug carriers for biomedical applications with prominent merits of biocompatibility and biodegradability. The encapsulation of PLNPs in liposomes renders the high drug loading efficiency, long-term NIR emission and remarkable therapeutic capabilities [122]. Mesoporous silica (MS) was another frequently used drug carrier. Zhao et al. showed MS-coated PLNPs with pH-driven targeting and cathepsin B/glutathione dual-responsive drug release capabilities for PL imaging and chemotherapy of tumor [123]. Feng et al. developed a raspberry-like mesoporous $Zn_{1.07}Ga_{2.34}Si_{0.98}O_{6.56}$:$Cr_{0.01}$ (Si-ZGO) nanocarriers for enhanced PL imaging and chemotherapy [124]. Metal–organic frameworks (MOFs) are advanced porous materials constructed by self-assembly of metal ions and multifunctional organic ligands, which have been widely used in separation, catalysis, molecular storage, biosensing/imaging and cancer therapy. The biocompatible porous framework ZIF-8 showed a significant drug loading capacity, which has been used as acidic triggered drug release platform for the efficient cancer chemotherapy. Zhao et al. and Lv et al. constructed a PLNPs@ZIF-8 core–shell multifunctional nanoplatform using different assemble steps and then loaded with doxorubicin (DOX). The tumor site-specific drug release and the persistent luminescence imaging were successfully achieved (Fig. 10) [125, 126]. Apart from these strategies, more efforts need to be made to improve the targeting and therapeutic efficiency [127].

5.2 PLNPs-Based Photodynamic Therapy

PDT is a treatment that uses photosensitizers along with light excitation to generate cytotoxic singlet oxygens ($^1O_2$) to kill cancer cells. Due to its low toxicity and minimal invasiveness to normal cells, it has become an alternative to the conventional therapeutic modality for variety of cancers. However, most photosensitizers for PDT need continuous activation by UV or visible light for a long time, leading to the limitation of the penetration depth in tissues and the

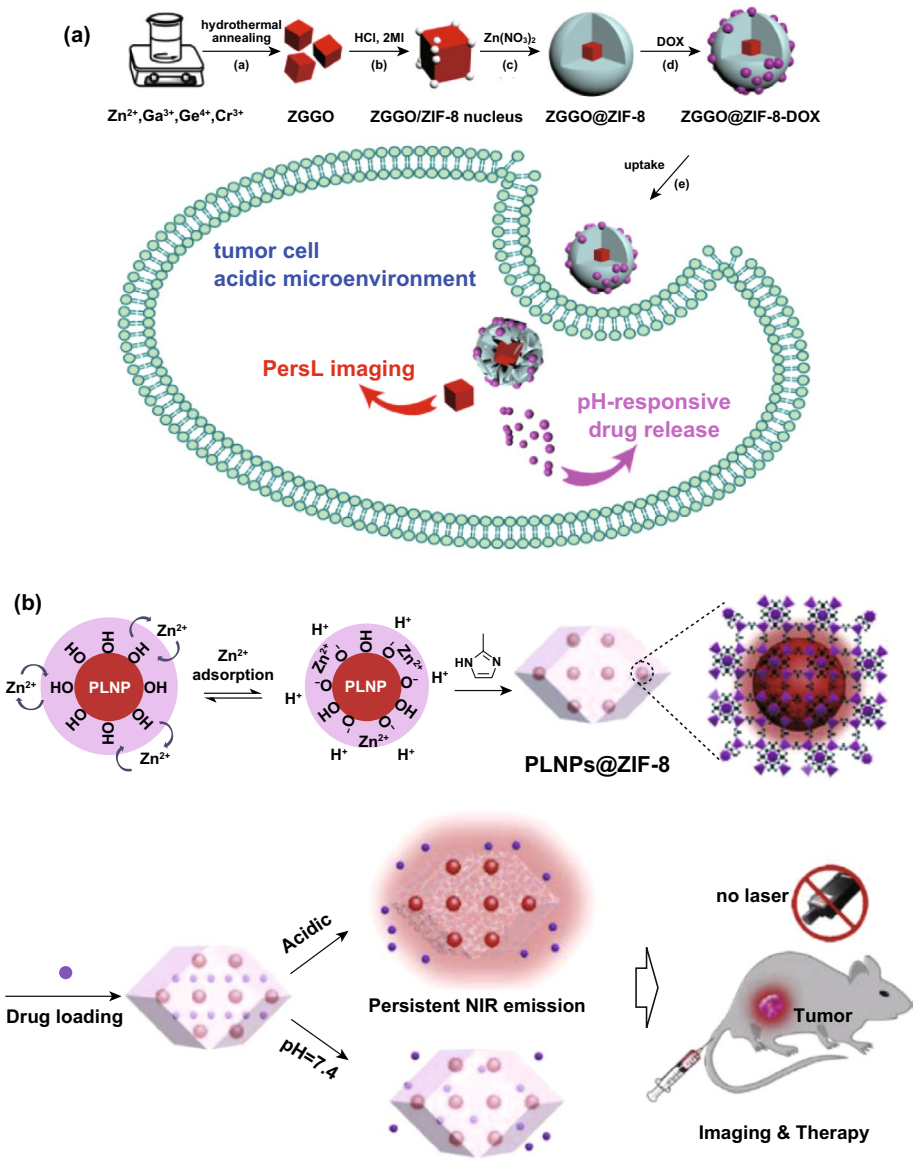

Fig. 10 **a** ZGGO@ZIF-8-DOX nanocomplex offered long-term NIR PL signals for the autofluorescence-free bioimaging and pH-responsive drug release for cancer chemotherapy. DOX release was accelerated in the acidic microenvironment of the tumor cells. Reproduced with permission from Ref. [125]. Copyright 2018 American Chemical Society. **b** PLNPs@ZIF-8 for acid-activated tumor imaging and drug release. Reproduced with permission from Ref. [126]. Copyright 2019 Elsevier Ltd

irradiation induced overheating and cell damages. PLNPs with long-lasting NIR emission can serve as a persistent light source for PDT activation without any need for continuous photonic excitation [128–130]. This promising feature can minimize the deleterious side effects of PDT and provide convenient clinical cancer treatment without continuous external irradiation [131–133].

Abdurahman and co-workers reported the photosensitizer (Si–Pc) covalently conjugated PLNPs with 808-nm NIR light renewable PL for PDT [131]. Except for covalent binding, Wang et al. [132] prepared a mesoporous silica shell for the photosensitizer (sulfonated aluminum phthalocyanine, a traditional photosensitizer) loading. Fan and co-workers constructed injectable PL implants as a built-in excitation source for an efficient repeatable PDT. This study represents a fresh concept of PLNPs-based PDT, leading to the efficient tumor growth suppression [134].

https://doi.org/10.1007/s40820-020-0404-8

5.3 PLNPs-Based Photothermal Therapy

In a typical PTT treatment, NIR light is converted into heat by proper agents (gold nanoparticles, CuS nanoparticles, graphene oxides, organic dyes, etc.), resulting in hyperthermia to kill cancer cells. Among the PTT agents, indocyanine green (ICG) is water-soluble and approved by FDA. To further improve the stability of ICG, several works about PLNPs functionalized with mesoporous silica shell have been developed to load ICG for the PL imaging-guided PTT [135–137]. Zheng and co-workers developed the PLNPs and ICG co-loaded mesoporous silica nanoparticles for PL imaging and PTT (Fig. 11). This new PTT agent could be used for significantly killing the cancer cells [135]. Chen et al. designed an activatable multifunctional PLNPs/CuS-based nanoplatform for PL imaging-guided PTT in vivo. CuS nanoparticles served as both PTT agent and the quencher with a high photothermal conversion efficiency and a strong NIR absorption. The prepared nanoprobes showed highly sensitive tumor-targeted PL imaging and effective PTT, leading to great potential for clinical theranostic applications [105].

5.4 Other Imaging-Guided Therapy

In some other cases, PLNPs were combined with other therapeutic agents for multiple applications. We first conjugated therapeutic plasmid on the polyetherimide (PEI)-modified PLNPs. The fabricated dual functional PLNPs can track the engineered mesenchymal stem cells (MSCs) homing and the gene therapy of glioblastoma [138]. Qin et al. [139] designed a gold nanorods/siRNA-assembled PLNPs nanofibers for LED-amplified gene silencing in cancer cells. The controllable integration of PLNPs with new functional groups also shows great potential for other clinical theranostic applications. For example, design of a vaccine/PLNPs-based nanocomposite for effective PL imaging-guided immune therapy was never reported so far [140, 141].

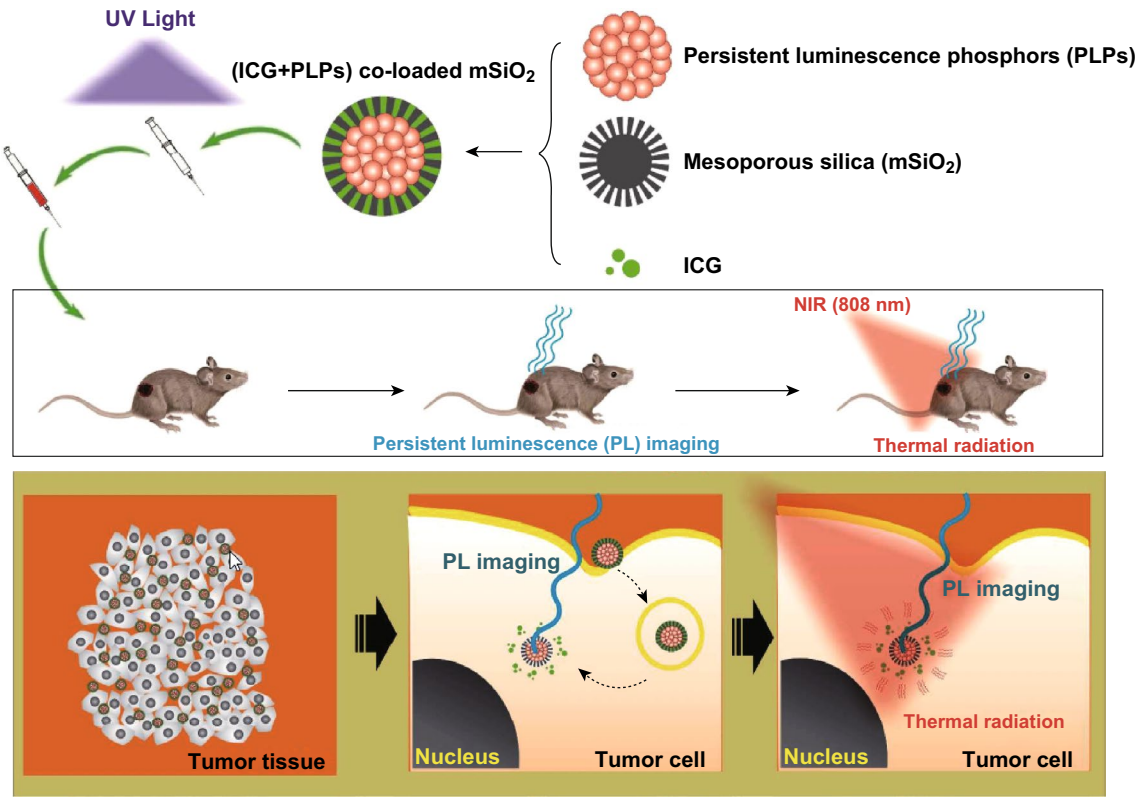

Fig. 11 Schematic representation shows the applications of ICG functionalized PLNPs for PL imaging-guided PTT in vivo. Reproduced with permission from Ref. [135]. Copyright 2016 American Chemical Society

6 Biodistribution and Biosafety Evaluations of PLNPs

A growing insight toward in vivo applications has led to major improvements in the evaluation of the biodistribution and biosafety of PLNPs. The influences of the crystal size, the surface modification, the layer thickness and the charge on the biodistribution of PLNPs after intravenous injection have been evaluated in living animals [121, 142, 143]. In general, the tissue distribution is found to be highly dependent on the surface coverage, as well as the core diameter. The PEG grafting is the most widely used surface modification method. It is found that increasing PEG chain length or density on the surface of PLNPs can significantly slow down the uptake process by RES. The precise control of PEG density can prevent protein adsorption on the surface of PLNPs and significantly reduce macrophage uptake in vitro [144]. Such promising results offer broad prospects for long-term applications of PLNPs in vivo.

Toxicity assessment of PLNPs is quite necessary for bioapplications [145, 146]. The in vitro or in vivo evaluation methods include the cytotoxicity study, the cell proliferation and differentiation, the physical and behavioral signs, the histological or hematological analysis, the hemolysis and blood biochemistry analysis and so on. The most convenient approach for evaluation of the cytotoxicity of PLNP is the cell viability test after PLNPs incubation. The impact of PLNPs on the cellular proliferative and differentiative ability is another important indicator of the cytotoxicity. We investigated the influence of PLNPs on the differentiation of adipose-derived stem cells (ASC) and human mesenchymal stem cells (MSCs) by culturing with adipogenic, chondrogenic and osteogenic supplemented medium, respectively. The microscopic images showed no significant stain difference between PLNPs labeled and unlabeled stem cells in each kind of differentiation. Consequently, these data suggest that PLNPs did not affect ASC and MSC differentiation [35, 138].

Physical and behavioral signs, such as the body weight, the excrement analysis, and behavior traits are employed to assess in vivo toxicity. The results generally indicate no significant changes as compared to the control groups [131]. In vivo toxicity of PLNPs is also evaluated via histological studies of main organs, including heart, liver, spleen, lung, kidney and other organs harvested from PLNPs pre-injected mice. The microscopic images of slices stained with hematoxylin and eosin (H&E) showed that PLNPs hardly caused any lesions, tissue damage or inflammation to organs [3, 98]. Ramírez-García and coworkers focused on several parameters, such as reactive oxygen species (ROS) indexes upon exposure to PLNPs, alterations in morphology at tissues and cellular levels and impact on blood cell counts [145, 146]. However, the currently obtained results of the biosafety evaluation of PLNPs are limited by relatively rudimentary and superficial methods. The possible immunotoxicity introduced by PLNPs needs further research in vivo. The relationship between the characteristics of PLNPs (composition, shape, size, surface modification, etc.) and toxicity needs to be systematically and profoundly established, especially for the long-term tracking studies.

7 New Organic and Polymeric PLNPs with Long Afterglow for In Vivo Optical Imaging

Nowadays, the number and type of PLNPs are still relatively limited. The main interest worldwide has focused on the rare earth heavy metal ions-doped inorganic materials. The high-cost, relatively complicated preparation and surface modification methods present the barriers for commercialization. Therefore, the development of new types of inexpensive, long-term emitting, biocompatible, eco-friendly and heavy metal ions-free afterglow materials is highly desirable [147–149]. Yang et al. reported a new type of metal–organic frameworks (MOFs) with long-lasting afterglow which showed highly tunable afterglow phosphorescence colors upon pyridine solution treatment. This finding supplies a group of MOFs-based persistent luminescence nanophosphors with high performance [150–154]. Up to now, the afterglow MOFs have not been used in biomedical fields in vivo due to the relatively short emission wavelength and the undesirable diameter.

In recent years, afterglow organic ingredients and polymers have captured special attention of chemist and biomedical scientists [155–157]. Semiconducting polymer nanoparticles (SPNs) assembled from completely benign organic components have emerged as versatile optical agents

https://doi.org/10.1007/s40820-020-0404-8

for molecular imaging [158–160]. Miao et al. presented the SPNs that can store the photo energy via chemical defects and emit NIR long persistent luminescence at 780 nm. The afterglow intensity of the SPNs show more than 100-fold brighter than that of inorganic PLNPs. SPNs were used for the lymph node and tumor imaging with a significant high SNR. Moreover, the developed SPNs-based probe can detect the early drug-induced hepatotoxicity in living mice [42]. Recently, He et al. have developed an organic afterglow protheranostic nanoassembly (APtN) with the afterglow imaging and the drug release in response to tumor microenvironment (excessive H_2O_2). Such molecular architecture combines passively tumor targeting, specific drug releasing and spontaneous afterglow generation, which provides design guidelines for activatable cancer theranostics (Fig. 12) [161–163].

The organic and polymeric PLNPs show high biocompatibility, good biodegradability and flexible synthesis and surface modification advantages for bioimaging and imaging-guided therapy. So far, there is rare report on the precise in-depth imaging-guided cancer surgery. Ni et al. synthesized a NIR PLNPs with aggregation-induced emission (AIE) characteristics. This AIE PLNPs showed innate property of fast PL signal quenching in normal tissues and gave ultrahigh tumor-to-liver signal ratio. These fascinating features make AIE PLNPs an excellent imaging-guided probe for peritoneal carcinomatosis resection (Fig. 13) [164].

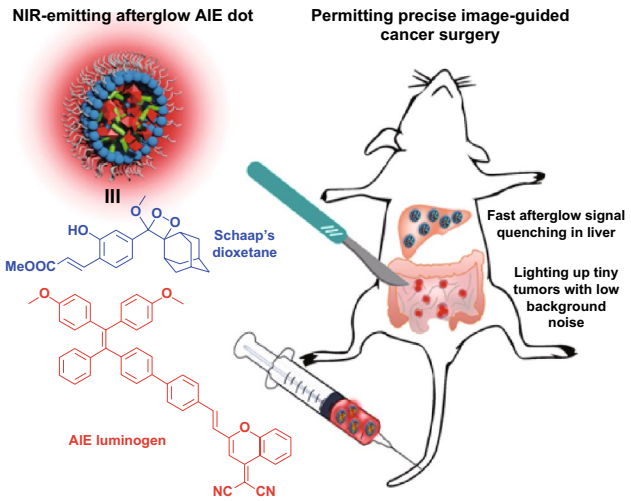

Fig. 13 NIR-emitting afterglow AIE dots for precise image-guided cancer surgery. Reproduced with permission from Ref. [164]. Copyright 2018 American Chemical Society

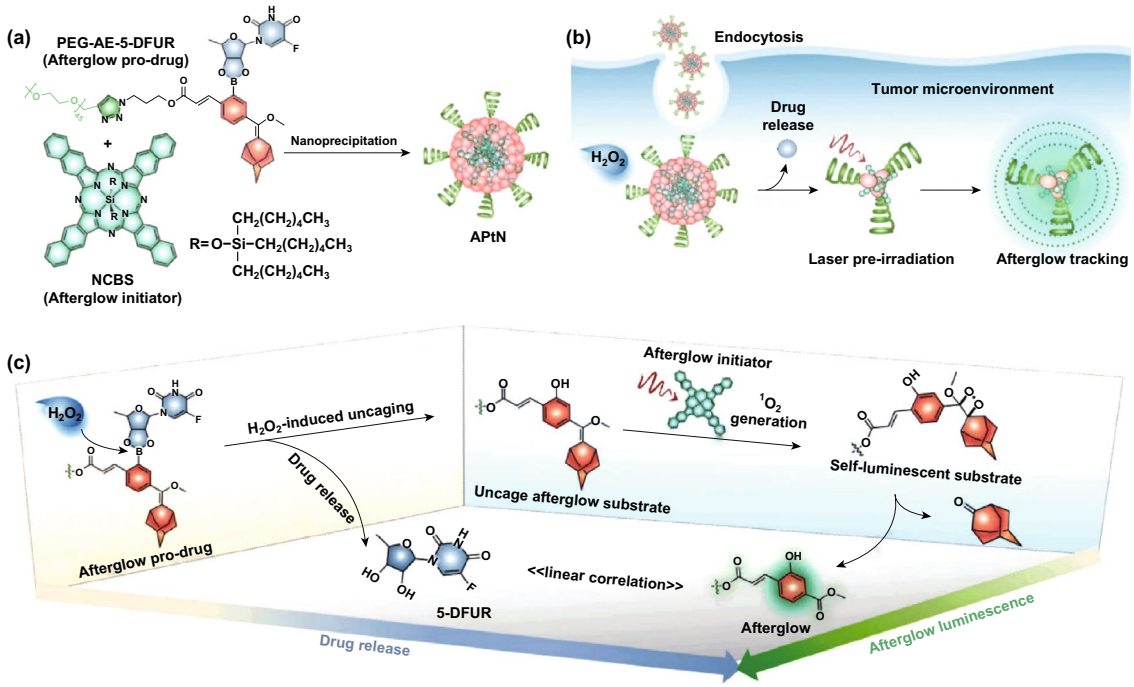

Fig. 12 **a** Design and synthesis of APtN. The chemical structures of the afterglow initiator (NCBS) and the afterglow pro-drug (PEG-AE-5-DFUR). **b**, **c** Tumor microenvironment responded drug release and laser irradiated $^1O_2$ generation and afterglow tracking. Reproduced with permission from Ref. [163]. Copyright 2019 WILEY–VCH Verlag GmbH & Co. KGaA, Weinheim

These new types of persistent luminescence nanophosphors with NIR emission, biocompatible and biodegradable nature have great promise as advanced molecular imaging tools, while the mechanism, synthesis methods, toxicity, imaging sensitivity and wide applications need further exploration and achievements.

8 Conclusion and Outlook

In this review, we provided a full-scale review of PLNPs from fundamental principles to all possible applications. The PLNPs possess a special advantage in eliminating autofluorescence interferences without constant in situ excitation, which is ideal for long-term bioapplication. We discussed the main and recent developments in the diagnostic and therapeutic applications of PLNPs, covering biosensing, multimodal imaging, drug delivery and imaging-guided therapy. In order to promote the biomedical applications of PLNPs, general and economic protocols for the synthesis and surface modification have been developed, which are optimized for bioapplications with high biocompatibility, stability and low toxicity. PLNPs with different composition have been widely designed to enhance the PL intensity and the decay time to achieve better in vivo imaging performance in the past decade, while, as shown above, not all of the reported routes can simultaneously control the shape, size and homogeneity of nanoparticles as well as the long persistent luminescence duration at the same time. The involved methods just partly improve the properties of PLNPs. Although rapid progress has been made in synthesis process, there are still many fields that need additional work, including controllable synthesis of PLNPs with new wavelength emission and excitation bands, improving phosphorescence lifetime and afterglow intensity, exploring new activators, matrices and novel multifunctional application fields.

Several pioneering works on investigating the biosensing applications of PLNPs have been reported. The PL-based biosensing can reveal analysis of biomolecules with superior SNR and high sensitivity in complicated biological samples. It is highly desirable to develop PLNPs-based bioprobes for monitoring other important biomolecules in vivo, such as the levels of toxins and signal molecules in the living body. PLNPs with multiple combinations and modifications offer more possibilities for incorporation with other imaging modalities (MRI, CT, PET, etc.). PL imaging-guided therapy can afford guiding cancer therapy with superior SNR. PLNPs can emit long persistent luminescence without continuous in situ external excitation and can act as the internal light source for imaging-guided therapy, avoiding the overheating and tissue damage caused by conventional photo-assisted therapies with constant light excitation (UV light, 808 nm light, etc.).

The various approaches for biosafety assessment of PLNPs have also been briefly studied. PLNPs show great promise in bioapplications without obvious toxicity. For clinical applications, more efforts need to be devoted beyond nanoplatform construction, such as efficacy, price, clinical safety and degradation. Very recently, Lécuyer et al. have studied the degradation of PLNPs in biological media mimicking solutions. They provided valuable information for the possible elimination of PLNPs after in vivo preclinical applications [165]. The PL imaging-guided tracking of the disease processes should also be studied in the future. We hope that this review could comprehensively summarize the properties and bioapplications of PLNPs and will shed new light on future directions to develop novel PLNPs and discover novel benefits for multiple applications.

Acknowledgements This work was supported by the National Natural Science Foundation of China (Nos. 21804109, 31771577), the China Postdoctoral Science Foundation (2018M633561), the Natural Science Basic Research Plan in Shaanxi Province of China (2019JQ-034, 2018JM3027), the Fundamental Research Funds for the Central Universities (G2018KY0304 and 3102017OQD047) and the National Undergraduate Training Programs for Innovation and Entrepreneurship (201810699376, 201810699344, 201910699028).

References

1. Y. Liu, J. Kuang, B. Lei, C. Shi, Color-control of long-lasting phosphorescence (LLP) through rare earth ion-doped cadmium metasilicate phosphors. J. Mater. Chem. **15**(37), 4025–4031 (2005). https://doi.org/10.1039/B507774E
2. Z. Pan, Y.-Y. Lu, F. Liu, Sunlight-activated long-persistent luminescence in the near-infrared from Cr^{3+}-doped zinc gallogermanates. Nat. Mater. **11**(1), 58–63 (2011). https://doi.org/10.1038/nmat3173
3. T. Maldiney, A. Bessière, J. Seguin, E. Teston, S.K. Sharma et al., The in vivo activation of persistent nanophosphors for optical imaging of vascularization, tumours and grafted cells. Nat. Mater. **13**(4), 418–426 (2014). https://doi.org/10.1038/nmat3908
4. J. Xu, J. Ueda, S. Tanabe, Toward tunable and bright deep-red persistent luminescence of Cr^{3+} in garnets. J. Am. Ceram. Soc. **100**(9), 4033–4044 (2017). https://doi.org/10.1111/jace.14942
5. T. Matsuzawa, Y. Aoki, N. Takeuchi, Y. Murayama, A new long phosphorescent phosphor with high brightness, $SrAl_2O_4$:Eu^{2+}, Dy^{3+}. J. Electrochem. Soc. **143**(8), 2670–2673 (1996). https://doi.org/10.1149/1.1837067
6. F. Chi, X. Wei, B. Jiang, Y. Chen, C. Duan, M. Yin, Luminescence properties and the thermal quenching mechanism of Mn^{2+} doped Zn_2GeO_4 long persistent phosphors. Dalton Trans. **47**(4), 1303–1311 (2018). https://doi.org/10.1039/c7dt03906a
7. O.Q. De Clercq, D. Poelman, Local, temperature-dependent trapping and detrapping in the $LiGa_5O_8$: Cr infrared emitting persistent phosphor. ECS J. Solid State Sci. Technol. **7**(1), 3171–3175 (2018). https://doi.org/10.1149/2.0211801jss
8. T. Lyu, P. Dorenbos, Charge carrier trapping processes in lanthanide doped $LaPO_4$, $GdPO_4$, YPO_4, and $LuPO_4$. J. Mater. Chem. C **6**(2), 369–379 (2018). https://doi.org/10.1039/c7tc05221a
9. I. Sahu, D.P. Bisen, K.V.R. Murthy, R.K. Tamrakar, Studies on the luminescence properties of cerium co-doping on $Ca_2MgSi_2O_7$:Eu^{2+} phosphor by solid-state reaction method. Luminescence **32**(7), 1263–1276 (2017). https://doi.org/10.1002/bio.3320
10. F. Liu, W. Yan, Y.-J. Chuang, Z. Zhen, J. Xie, Z. Pan, Photostimulated near-infrared persistent luminescence as a new optical read-out from Cr^{3+}-doped $LiGa_5O_8$. Sci. Rep. **3**(1), 1554 (2013). https://doi.org/10.1038/srep01554
11. M. Allix, S. Chenu, E. Véron, T. Poumeyrol, E. Kouadri-Boudjelthia, S. Alahraché, F. Porcher, D. Massiot, F. Fayon, Considerable improvement of long-persistent luminescence in germanium and tin substituted $ZnGa_2O_4$. Chem. Mater. **25**(9), 1600–1606 (2013). https://doi.org/10.1021/cm304101n
12. M. Sun, Z.-J. Li, C.-L. Liu, H.-X. Fu, J.-S. Shen, H.-W. Zhang, Persistent luminescent nanoparticles for super-long time in vivo and in situ imaging with repeatable excitation. J. Lumin. **145**, 838–842 (2014). https://doi.org/10.1016/j.jlumin.2013.08.070
13. S.K. Sharma, D. Gourier, B. Viana, T. Maldiney, E. Teston, D. Scherman, C. Richard, Persistent luminescence of AB_2O_4:Cr^{3+} (A = Zn, Mg, B = Ga, Al) spinels: new biomarkers for in vivo imaging. Opt. Mater. **36**(11), 1901–1906 (2014). https://doi.org/10.1016/j.optmat.2014.06.020
14. T. Maldiney, G. Sraiki, B. Viana, D. Gourier, C. Richard et al., In vivo optical imaging with rare earth doped $Ca_2Si_5N_8$ persistent luminescence nanoparticles. Opt. Mater. Express **2**(3), 261–268 (2012). https://doi.org/10.1364/OME.2.000261
15. C. Rosticher, B. Viana, T. Maldiney, C. Richard, C. Chanéac, Persistent luminescence of Eu, Mn, Dy doped calcium phosphates for in vivo optical imaging. J. Lumin. **170**, 460–466 (2016). https://doi.org/10.1016/j.jlumin.2015.07.024
16. M. Pellerin, E. Glais, T. Lecuyer, J. Xu, J. Seguin, S. Tanabe, C. Chanéac, B. Viana, C. Richard, $LaAlO_3$:Cr^{3+}, Sm^{3+}: nano-perovskite with persistent luminescence for in vivo optical imaging. J. Lumin. **202**, 83–88 (2018). https://doi.org/10.1016/j.jlumin.2018.05.024
17. C. Shi, Y. Zhu, G. Zhu, X. Shen, M. Ge, Phototunable full-color emission of dynamic luminescent materials. J. Mater. Chem. C **6**(35), 9552–9560 (2018). https://doi.org/10.1039/c8tc02955e
18. H. Lin, G. Bai, T. Yu, M.K. Tsang, Q. Zhang, J. Hao, Site occupancy and near-infrared luminescence in $Ca_3Ga_2Ge_3O_{12}$:Cr^{3+} persistent phosphor. Adv. Opt. Mater. **5**(18), 1700227 (2017). https://doi.org/10.1002/adom.201700227
19. F. Xue, Y. Hu, L. Fan, G. Ju, Y. Lv, Y. Li, Cr^{3+}-activated $Li_5Zn_8Al_5Ge_9O_{36}$: a near-infrared long-afterglow phosphor. J. Am. Ceram. Soc. **100**(7), 3070–3079 (2017). https://doi.org/10.1111/jace.14874
20. I. Norrbo, J.M. Carvalho, P. Laukkanen, J. Mäkelä, F. Mamedov et al., Lanthanide and heavy metal free long white persistent luminescence from Ti doped Li-hackmanite: a versatile, low-cost material. Adv. Funct. Mater. **27**(17), 1606547 (2017). https://doi.org/10.1002/adfm.201606547
21. T. Tu, G. Jiang, Enhanced persistent luminescence of Li_2ZnGeO_4 host by rare-earth ions (Pr^{3+}, Nd^{3+} and Gd^{3+}) doping. J. Mater. Sci. Mater. El. **29**(4), 3146–3152 (2017). https://doi.org/10.1007/s10854-017-8247-x
22. P. Ge, K. Sun, Y. Cheng, Design and synthesis of up-converted persistent luminescence $Zn_3Ga_2SnO_8$:Cr^{3+}, Yb^{3+}, Er^{3+} phosphor. Optik **188**, 200–204 (2019). https://doi.org/10.1016/j.ijleo.2019.05.011
23. F. Liu, Y. Liang, Z. Pan, Detection of up-converted persistent luminescence in the near infrared emitted by the $Zn_3Ga_2GeO_8$:Cr^{3+}, Yb^{3+}, Er^{3+} phosphor. Phys. Rev. Lett. **113**(17), 177401 (2014). https://doi.org/10.1103/PhysRevLett.113.177401
24. Z. Li, L. Huang, Y. Zhang, Y. Zhao, H. Yang, G. Han, Near-infrared light activated persistent luminescence nanoparticles via upconversion. Nano Res. **10**(5), 1840–1846 (2017). https://doi.org/10.1007/s12274-017-1548-9
25. Z. Xue, X. Li, Y. Li, M. Jiang, G. Ren, H. Liu, S. Zeng, J. Hao, A 980 nm laser-activated upconverted persistent probe

for NIR-to-NIR rechargeable in vivo bioimaging. Nanoscale **9**(21), 7276–7283 (2017). https://doi.org/10.1039/C6NR09716B

26. Y. Zhuang, Y. Lv, L. Wang, W. Chen, T.L. Zhou, T. Takeda, N. Hirosaki, R.J. Xie, Trap depth engineering of $SrSi_2O_2N_2$:Ln^{2+}, Ln^{3+} (Ln^{2+} = Yb, Eu; Ln^{3+} = Dy, Ho, Er) persistent luminescence materials for information storage applications. ACS Appl. Mater. Interfaces **10**(2), 1854–1864 (2018). https://doi.org/10.1021/acsami.7b17271
27. Y. Zhuang, L. Wang, Y. Lv, T.-L. Zhou, R.-J. Xie, Optical data storage and multicolor emission readout on flexible films using deep-trap persistent luminescence materials. Adv. Funct. Mater. **28**(8), 1705769 (2018). https://doi.org/10.1002/adfm.201705769
28. X. Liu, Q. Ji, Q. Hu, C. Li, M. Chen, J. Sun, Y. Wang, Q. Sun, B. Geng, Dual-mode long-lived luminescence of Mn^{2+}-doped nanoparticles for multilevel anticounterfeiting. ACS Appl. Mater. Interfaces **11**(33), 30146–30153 (2019). https://doi.org/10.1021/acsami.9b09612
29. T. Lecuyer, E. Teston, G. Ramirez-Garcia, T. Maldiney, B. Viana, J. Seguin, N. Mignet, D. Scherman, C. Richard, Chemically engineered persistent luminescence nanoprobes for bioimaging. Theranostics **6**(13), 2488–2524 (2016). https://doi.org/10.7150/thno.16589
30. J. Liu, T. Lécuyer, J. Séguin, N. Mignet, D. Scherman, B. Viana, C. Richard, Imaging and therapeutic applications of persistent luminescence nanomaterials. Adv. Drug Deliv. Rev. **138**, 193–210 (2019). https://doi.org/10.1016/j.addr.2018.10.015
31. K.Y. Zhang, Q. Yu, H. Wei, S. Liu, Q. Zhao, W. Huang, Long-lived emissive probes for time-resolved photoluminescence bioimaging and biosensing. Chem. Rev. **118**(4), 1770–1839 (2018). https://doi.org/10.1021/acs.chemrev.7b00425
32. D. Jia, L.A. Lewis, X.-J. Wang, Cr^{3+}-doped lanthanum gallogermanate phosphors with long persistent IR emission. Electrochem. Solid-St. **13**(4), J32–J34 (2010). https://doi.org/10.1149/1.3294520
33. A. Abdukayum, J.-T. Chen, Q. Zhao, X.-P. Yan, Functional near infrared-emitting Cr^{3+}/Pr^{3+} co-doped zinc gallogermanate persistent luminescent nanoparticles with superlong afterglow for in vivo targeted bioimaging. J. Am. Chem. Soc. **135**(38), 14125–14133 (2013). https://doi.org/10.1021/ja404243v
34. Y.J. Li, X.P. Yan, Synthesis of functionalized triple-doped zinc gallogermanate nanoparticles with superlong near-infrared persistent luminescence for long-term orally administrated bioimaging. Nanoscale **8**(32), 14965–14970 (2016). https://doi.org/10.1039/c6nr04950h
35. S.-Q. Wu, C.-W. Chi, C.-X. Yang, X.-P. Yan, Penetrating peptide-bioconjugated persistent nanophosphors for long-term tracking of adipose-derived stem cells with superior signal-to-noise ratio. Anal. Chem. **88**(7), 4114–4121 (2016). https://doi.org/10.1021/acs.analchem.6b00449
36. A. Verma, A. Verma, Synthesis, characterization, mechano-luminescence, thermoluminescence, and antibacterial properties of $SrMgAl_{10}O_{17}$:Eu phosphor. J. Alloys Compd. **802**, 394–408 (2019). https://doi.org/10.1016/j.jallcom.2019.06.209
37. Z. Li, Q. Wang, Y. Wang, Q. Ma, J. Wang, Z. Li, Y. Li, X. Lv, W. Wei, L. Chen, Q. Yuan, Background-free latent fingerprint imaging based on nanocrystals with long-lived luminescence and pH-guided recognition. Nano Res. **11**(12), 6167–6176 (2018). https://doi.org/10.1007/s12274-018-2133-6
38. A. Tuerdi, A. Abdukayum, Dual-functional persistent luminescent nanoparticles with enhanced persistent luminescence and photocatalytic activity. RSC Adv. **9**(31), 17653–17657 (2019). https://doi.org/10.1039/c9ra02235j
39. J. Xu, D. Murata, J. Ueda, S. Tanabe, Near-infrared long persistent luminescence of Er^{3+} in garnet for the third bioimaging window. J. Mater. Chem. C **4**(47), 11096–11103 (2016). https://doi.org/10.1039/c6tc04027f
40. J. Nie, Y. Li, S. Liu, Q. Chen, Q. Xu, J. Qiu, Tunable long persistent luminescence in the second near-infrared window via crystal field control. Sci. Rep. **7**(1), 12392 (2017). https://doi.org/10.1038/s41598-017-12591-1
41. R. Kabe, C. Adachi, Organic long persistent luminescence. Nature **550**(7676), 384–387 (2017). https://doi.org/10.1038/nature24010
42. Q. Miao, C. Xie, X. Zhen, Y. Lyu, H. Duan, X. Liu, J.V. Jokerst, K. Pu, Molecular afterglow imaging with bright, biodegradable polymer nanoparticles. Nat. Biotechnol. **35**(11), 1102–1110 (2017). https://doi.org/10.1038/nbt.3987
43. T. Maldiney, B.T. Doan, D. Alloyeau, M. Bessodes, D. Scherman, C. Richard, Gadolinium-doped persistent nanophosphors as versatile tool for multimodal in vivo imaging. Adv. Funct. Mater. **25**(2), 331–338 (2015). https://doi.org/10.1002/adfm.201401612
44. J. Wang, Q. Ma, X.-X. Hu, H. Liu, W. Zheng, X. Chen, Q. Yuan, W. Tan, Autofluorescence-free targeted tumor imaging based on luminous nanoparticles with composition-dependent size and persistent luminescence. ACS Nano **11**, 8010–8017 (2017). https://doi.org/10.1021/acsnano.7b02643
45. J. Wang, Q. Ma, Y. Wang, H. Shen, Q. Yuan, Recent progress in biomedical applications of persistent luminescence nanoparticles. Nanoscale **9**(19), 6204–6218 (2017). https://doi.org/10.1039/c7nr01488k
46. S.K. Sun, H.F. Wang, X.P. Yan, Engineering persistent luminescence nanoparticles for biological applications: from biosensing/bioimaging to theranostics. Acc. Chem. Res. **51**(5), 1131–1143 (2018). https://doi.org/10.1021/acs.accounts.7b00619
47. L. Liang, N. Chen, Y. Jia, Q. Ma, J. Wang, Q. Yuan, W. Tan, Recent progress in engineering near-infrared persistent luminescence nanoprobes for time-resolved biosensing/bioimaging. Nano Res. **12**(6), 1279–1292 (2019). https://doi.org/10.1007/s12274-019-2343-6
48. D. Jia, R.S. Meltzer, W.M. Yen, W. Jia, X. Wang, Green phosphorescence of $CaAl_2O_4$:Tb^{3+}, Ce^{3+} through persistence energy transfer. Appl. Phys. Lett. **80**(9), 1535–1537 (2002). https://doi.org/10.1063/1.1456955
49. S. Ye, J. Zhang, X. Zhang, S. Lu, X. Ren, X.-J. Wang, Mn^{2+} activated red phosphorescence in $BaMg_2Si_2O_7$: Mn^{2+}, Eu^{2+},

 https://doi.org/10.1007/s40820-020-0404-8

Dy^{3+} through persistent energy transfer. J. Appl. Phys. **101**(6), 063545 (2007). https://doi.org/10.1063/1.2714498

50. E. Teston, S. Richard, T. Maldiney, N. Lièvre, G. Wang, L. Motte, C. Richard, Y. Lalatonne, Non-aqueous sol–gel synthesis of ultra small persistent luminescence nanoparticles for near-infrared in vivo imaging. Chem. Eur. J. **21**(20), 7350–7354 (2015). https://doi.org/10.1002/chem.201406599
51. D. Jia, X.J. Wang, W. Jia, W.M. Yen, Persistent energy transfer in $CaAl_2O_4$:Tb^{3+}, Ce^{3+}. J. Appl. Phys. **93**(1), 148–152 (2003). https://doi.org/10.1063/1.1525860
52. R. Zhong, J. Zhang, X. Zhang, S. Lu, X.-J. Wang, Red phosphorescence in $Sr_4Al_{14}O_{25}$: Cr^{3+}, Eu^{2+}, Dy^{3+} through persistent energy transfer. Appl. Phys. Lett. **88**(20), 201916 (2006). https://doi.org/10.1063/1.2205167
53. Z.-J. Li, Y.-J. Zhang, H.-W. Zhang, H.-X. Fu, Long-lasting phosphorescence functionalization of mesoporous silica nanospheres by $CaTiO_3$:Pr^{3+} for drug delivery. Micropor. Mesopor. Mat. **176**, 48–54 (2013). https://doi.org/10.1016/j.micromeso.2013.02.050
54. Z. Li, Y. Zhang, X. Wu, L. Huang, D. Li, W. Fan, G. Han, Direct aqueous-phase synthesis of sub-10 nm "luminous pearls" with enhanced in vivo renewable near-infrared persistent luminescence. J. Am. Chem. Soc. **137**(16), 5304–5307 (2015). https://doi.org/10.1021/jacs.5b00872
55. H. Liu, X. Hu, J. Wang, M. Liu, W. Wei, Q. Yuan, Direct low-temperature synthesis of ultralong persistent luminescence nanobelts based on a biphasic solution-chemical reaction. Chinese Chem. Lett. **29**(11), 1641–1644 (2018). https://doi.org/10.1016/j.cclet.2018.02.005
56. E. Bonturim, L.G. Merízio, R. dos Reis, H.F. Brito, L.C.V. Rodrigues, M.C.F.C. Felinto, Persistent luminescence of inorganic nanophosphors prepared by wet-chemical synthesis. J. Alloys Compd. **732**, 705–715 (2018). https://doi.org/10.1016/j.jallcom.2017.10.219
57. P. Liu, Y. Liu, C. Cui, L. Wang, J. Qiao, P. Huang, Q. Shi, Y. Tian, H. Jiang, J. Jiang, Enhanced luminescence and afterglow by heat-treatment in reducing atmosphere to synthesize the $Gd_3Al_2Ga_3O_{12}$: Ce^{3+} persistent phosphor for acleds. J. Alloys Compd. **731**, 389–396 (2018). https://doi.org/10.1016/j.jallcom.2017.10.037
58. A.S. Maia, R. Stefani, C.A. Kodaira, M. Felinto, E. Teotonio, H.F. Brito, Luminescent nanoparticles of $MgAl_2O_4$:Eu, Dy prepared by citrate sol–gel method. Opt. Mater. **31**(2), 440–444 (2008). https://doi.org/10.1016/j.optmat.2008.06.017
59. T. Maldiney, B. Viana, A. Bessière, D. Gourier, M. Bessodes, D. Scherman, C. Richard, In vivo imaging with persistent luminescence silicate-based nanoparticles. Opt. Mater. **35**(10), 1852–1858 (2013). https://doi.org/10.1016/j.optmat.2013.03.028
60. F. Ye, S. Dong, Z. Tian, S. Yao, Z. Zhou, S. Wang, Fabrication of the PLA/$Sr_2MgSi_2O_7$:Eu^{2+}, Dy^{3+} long-persistent luminescence composite fibers by electrospinning. Opt. Mater. **36**(2), 463–466 (2013). https://doi.org/10.1016/j.optmat.2013.10.019
61. Z. Li, H. Zhang, M. Sun, J. Shen, H. Fu, A facile and effective method to prepare long-persistent phosphorescent nanospheres and its potential application for in vivo imaging. J. Mater. Chem. **22**(47), 24713–24720 (2012). https://doi.org/10.1039/C2JM35650C
62. Z. Li, J. Shi, H. Zhang, M. Sun, Highly controllable synthesis of near-infrared persistent luminescence SiO_2/$CaMgSi_2O_6$ composite nanospheres for imaging in vivo. Opt. Express **22**(9), 10509 (2014). https://doi.org/10.1364/OE.22.010509
63. J. Shi, M. Sun, X. Sun, H. Zhang, Near-infrared persistent luminescence hollow mesoporous nanospheres for drug delivery and in vivo renewable imaging. J. Mater. Chem. B **4**(48), 7845–7851 (2016). https://doi.org/10.1039/C6TB02674E
64. J. Shi, X. Sun, J. Li, H. Man, J. Shen, Y. Yu, H. Zhang, Multifunctional near infrared-emitting long-persistence luminescent nanoprobes for drug delivery and targeted tumor imaging. Biomaterials **37**, 260–270 (2015). https://doi.org/10.1016/j.biomaterials.2014.10.033
65. B.B. Srivastava, A. Kuang, Y. Mao, Persistent luminescent sub-10 nm Cr doped $ZnGa_2O_4$ nanoparticles by a biphasic synthesis route. Chem. Commun. **51**(34), 7372–7375 (2015). https://doi.org/10.1039/c5cc00377f
66. J.-L. Li, J.-P. Shi, C.-C. Wang, P.-H. Li, Z.-F. Yu, H.-W. Zhang, Five-nanometer $ZnSn_2O_4$:Cr, Eu ultra-small nanoparticles as new near infrared-emitting persistent luminescent nanoprobes for cellular and deep tissue imaging at 800 nm. Nanoscale **9**(25), 8631–8638 (2017). https://doi.org/10.1039/c7nr02468a
67. R. Zou, J. Huang, J. Shi, L. Huang, X. Zhang et al., Silica shell-assisted synthetic route for mono-disperse persistent nanophosphors with enhanced in vivo recharged near-infrared persistent luminescence. Nano Res. **10**(6), 2070–2082 (2016). https://doi.org/10.1007/s12274-016-1396-z
68. J. Yang, Y. Liu, D. Yan, H. Zhu, C. Liu, C. Xu, L. Ma, X. Wang, A vacuum-annealing strategy for improving near-infrared super long persistent luminescence in Cr^{3+} doped zinc gallogermanate nanoparticles for bio-imaging. Dalton T. **45**(4), 1364–1372 (2016). https://doi.org/10.1039/c5dt03875h
69. T. Maldiney, M.U. Kaikkonen, J. Seguin, Q. le Masne de Chermont, M. Bessodes et al., In vitro targeting of avidin-expressing glioma cells with biotinylated persistent luminescence nanoparticles. Bioconjug. Chem. **23**(3), 472–478 (2012). https://doi.org/10.1021/bc200510z
70. J. Wang, J. Li, J. Yu, H. Zhang, B. Zhang, Large hollow cavity luminous nanoparticles with near-infrared persistent luminescence and tunable sizes for tumor afterglow imaging and chemo-/photodynamic therapies. ACS Nano **12**(5), 4246–4258 (2018). https://doi.org/10.1021/acsnano.7b07606
71. J. Wang, Q. Ma, X.X. Hu, H. Liu, W. Zheng, X. Chen, Q. Yuan, W. Tan, Autofluorescence-free targeted tumor imaging based on luminous nanoparticles with composition-dependent size and persistent luminescence. ACS Nano **11**(8), 8010–8017 (2017). https://doi.org/10.1021/acsnano.7b02643

72. H.F. Wang, X. Chen, F. Feng, X. Ji, Y. Zhang, Edta etching: a simple way for regulating the traps, size and aqueous-dispersibility of Cr^{3+}-doped zinc gallate. Chem. Sci. **9**(48), 8923–8929 (2018). https://doi.org/10.1039/c8sc04173c
73. Y.J. Li, C.X. Yang, X.P. Yan, Biomimetic persistent luminescent nanoplatform for autofluorescence-free metastasis tracking and chemophotodynamic therapy. Anal. Chem. **90**(6), 4188–4195 (2018). https://doi.org/10.1021/acs.analchem.8b00311
74. J.M. Liu, D.D. Zhang, G.Z. Fang, S. Wang, Erythrocyte membrane bioinspired near-infrared persistent luminescence nanocarriers for in vivo long-circulating bioimaging and drug delivery. Biomaterials **165**, 39–47 (2018). https://doi.org/10.1016/j.biomaterials.2018.02.042
75. Z.H. Wang, J.M. Liu, C.Y. Li, D. Wang, H. Lv, S.W. Lv, N. Zhao, H. Ma, S. Wang, Bacterial biofilm bioinspired persistent luminescence nanoparticles with gut-oriented drug delivery for colorectal cancer imaging and chemotherapy. ACS Appl. Mater. Interfaces **11**(40), 36409–36419 (2019). https://doi.org/10.1021/acsami.9b12853
76. X. Zhao, L.-J. Chen, K.-C. Zhao, Y.-S. Liu, J.-L. Liu, X.-P. Yan, Autofluorescence-free chemo/biosensing in complex matrixes based on persistent luminescence nanoparticles. TrAC Trend. Anal. Chem. **118**, 65–72 (2019). https://doi.org/10.1016/j.trac.2019.05.025
77. B.Y. Wu, H.F. Wang, J.T. Chen, X.P. Yan, Fluorescence resonance energy transfer inhibition assay for alpha-fetoprotein excreted during cancer cell growth using functionalized persistent luminescence nanoparticles. J. Am. Chem. Soc. **133**(4), 686–688 (2011). https://doi.org/10.1021/ja108788p
78. N. Li, Y. Li, Y. Han, W. Pan, T. Zhang, B. Tang, A highly selective and instantaneous nanoprobe for detection and imaging of ascorbic acid in living cells and in vivo. Anal. Chem. **86**(8), 3924–3930 (2014). https://doi.org/10.1021/ac5000587
79. N. Li, W. Diao, Y. Han, W. Pan, T. Zhang, B. Tang, MnO_2-modified persistent luminescence nanoparticles for detection and imaging of glutathione in living cells and in vivo. Chem. Eur. J. **20**(50), 16488–16491 (2014). https://doi.org/10.1002/chem.201404625
80. L. Zhang, J. Lei, J. Liu, F. Ma, H. Ju, Persistent luminescence nanoprobe for biosensing and lifetime imaging of cell apoptosis via time-resolved fluorescence resonance energy transfer. Biomaterials **67**, 323–334 (2015). https://doi.org/10.1016/j.biomaterials.2015.07.037
81. B.Y. Wu, X.P. Yan, Bioconjugated persistent luminescence nanoparticles for foster resonance energy transfer immunoassay of prostate specific antigen in serum and cell extracts without in situ excitation. Chem. Commun. **51**(18), 3903–3906 (2015). https://doi.org/10.1039/c5cc00286a
82. Y. Wang, Z. Li, Q. Lin, Y. Wei, J. Wang, Y. Li, R. Yang, Q. Yuan, Highly sensitive detection of bladder cancer-related miRNA in urine using time-gated luminescent biochip. ACS Sensors **4**(8), 2124–2130 (2019). https://doi.org/10.1021/acssensors.9b00927
83. J. Tang, Y. Su, D. Deng, L. Zhang, N. Yang, Y. Lv, A persistent luminescence microsphere-based probe for convenient imaging analysis of dopamine. Analyst **141**(18), 5366–5373 (2016). https://doi.org/10.1039/c6an00882h
84. Y. Liu, J.M. Liu, D. Zhang, K. Ge, P. Wang, H. Liu, G. Fang, S. Wang, Persistent luminescence nanophosphor involved near-infrared optical bioimaging for investigation of food-borne probiotics biodistribution in vivo: a proof-of-concept study. J. Agr. Food Chem. **65**(37), 8229–8240 (2017). https://doi.org/10.1021/acs.jafc.7b02870
85. J. Yang, Y. Liu, Y. Zhao, Z. Gong, M. Zhang et al., Ratiometric afterglow nanothermometer for simultaneous in situ bioimaging and local tissue temperature sensing. Chem. Mater. **29**(19), 8119–8131 (2017). https://doi.org/10.1021/acs.chemmater.7b01958
86. Z. Zhou, W. Zheng, J. Kong, Y. Liu, P. Huang, S. Zhou, Z. Chen, J. Shi, X. Chen, Rechargeable and led-activated $ZnGa_2O_4$:Cr^{3+} near-infrared persistent luminescence nanoprobes for background-free biodetection. Nanoscale **9**(20), 6846–6853 (2017). https://doi.org/10.1039/c7nr01209h
87. A.S. Paterson, B. Raja, G. Garvey, A. Kolhatkar, A.E. Hagstrom, K. Kourentzi, T.R. Lee, R.C. Willson, Persistent luminescence strontium aluminate nanoparticles as reporters in lateral flow assays. Anal. Chem. **86**(19), 9481–9488 (2014). https://doi.org/10.1021/ac5012624
88. Q. le Masne de Chermont, C. Chanéac, J. Seguin, F. Pellé, S. Maîtrejean, J.P. Jolivet, D. Gourier, M. Bessodes, D. Scherman, Nanoprobes with near-infrared persistent luminescence for in vivo imaging. PNAS **104**(22), 9266–9271 (2007). https://doi.org/10.1073/pnas.0702427104
89. X. Sun, J. Shi, S. Zheng, J. Li, S. Wang, H. Zhang, Visualization of inflammation in a mouse model based on near-infrared persistent luminescence nanoparticles. J. Lumin. **204**, 520–527 (2018). https://doi.org/10.1016/j.jlumin.2018.08.058
90. D.D. Zhang, J.M. Liu, S.M. Sun, C. Liu, G.Z. Fang, S. Wang, Construction of persistent luminescence-plastic antibody hybrid nanoprobe for in vivo recognition and clearance of pesticide using background-free nanobioimaging. J. Agr. Food Chem. **67**(24), 6874–6883 (2019). https://doi.org/10.1021/acs.jafc.9b02712
91. Y.-J. Chuang, Z. Zhen, F. Zhang, F. Liu, J.P. Mishra et al., Photostimulable near-infrared persistent luminescent nanoprobes for ultrasensitive and longitudinal deep-tissue bioimaging. Theranostics **4**(11), 1112–1122 (2014). https://doi.org/10.7150/thno.9710
92. B. Can-Uc, J.B. Montes-Frausto, K. Juarez-Moreno, J. Licea-Rodriguez, I. Rocha-Mendoza, G.A. Hirata, Light sheet microscopy and $SrAl_2O_4$ nanoparticles codoped with Eu^{2+}/Dy^{3+} ions for cancer cell tagging. J. Biophotonics **11**(6), e201700301 (2018). https://doi.org/10.1002/jbio.201700301
93. E. Teston, T. Maldiney, I. Marangon, J. Volatron, Y. Lalatonne et al., Nanohybrids with magnetic and persistent luminescence properties for cell labeling, tracking, in vivo real-time imaging, and magnetic vectorization. Small **14**(16), e1800020 (2018). https://doi.org/10.1002/smll.201800020

 https://doi.org/10.1007/s40820-020-0404-8

94. L.J. Chen, X. Zhao, X.P. Yan, Cell-penetrating peptide-functionalized persistent luminescence nanoparticles for tracking J774A.1 macrophages homing to inflamed tissues. ACS Appl. Mater. Interfaces **11**(22), 19894–19901 (2019). https://doi.org/10.1021/acsami.9b05870
95. J.M. Liu, N. Zhao, Z.H. Wang, S.W. Lv, C.Y. Li, S. Wang, In-taken labeling and in vivo tracing foodborne probiotics via DNA-encapsulated persistent luminescence nanoprobe assisted autofluorescence-free bioimaging. J. Agr. Food Chem. **67**(1), 514–519 (2019). https://doi.org/10.1021/acs.jafc.8b05937
96. H. Liu, F. Ren, X. Zhou, C. Ma, T. Wang, H. Zhang, Q Sun., Z. Li, Ultra-sensitive detection and inhibition of the metastasis of breast cancer cells to adjacent lymph nodes and distant organs by using long-persistent luminescence nanoparticles. Anal. Chem. **91**(23), 15064–15072 (2019). https://doi.org/10.1021/acs.analchem.9b03739
97. H. Zhao, C. Liu, Z. Gu, L. Dong, F. Li, C. Yao, D. Yang, Persistent luminescent nanoparticles containing hydrogels for targeted, sustained, and autofluorescence-free tumor metastasis imaging. Nano Lett. **20**(1), 252–260 (2020). https://doi.org/10.1021/acs.nanolett.9b03755
98. H.-X. Zhao, C.-X. Yang, X.-P. Yan, Fabrication and bioconjugation of B^{III} and Cr^{III} co-doped $ZnGa_2O_4$ persistent luminescent nanoparticles for dual-targeted cancer bioimaging. Nanoscale **8**(45), 18987–18994 (2016). https://doi.org/10.1039/C6NR06259H
99. A. Abdukayum, C.-X. Yang, Q. Zhao, J.-T. Chen, L.-X. Dong, X.-P. Yan, Gadolinium complexes functionalized persistent luminescent nanoparticles as a multimodal probe for near-infrared luminescence and magnetic resonance imagingin vivo. Anal. Chem. **86**(9), 4096–4101 (2014). https://doi.org/10.1021/ac500644x
100. Z. Gong, J. Yang, H. Zhu, D. Yan, C. Liu, C. Xu, Y. Liu, The synergistically improved afterglow and magnetic resonance imaging induced by Gd^{3+} doping in ZGGO:Cr^{3+} nanoparticles. Mater. Res. Bull. **113**, 122–132 (2019). https://doi.org/10.1016/j.materresbull.2019.01.031
101. J. Shi, H. Fu, X. Sun, J. Shen, H. Zhang, Magnetic, long persistent luminescent and mesoporous nanoparticles as trackable transport drug carriers. J. Mater. Chem. B **3**(4), 635–641 (2014). https://doi.org/10.1039/C4TB01721H
102. E. Teston, Y. Lalatonne, D. Elgrabli, G. Autret, L. Motte et al., Design, properties, and in vivo behavior of super-paramagnetic persistent luminescence nanohybrids. Small **11**(22), 2696–2704 (2015). https://doi.org/10.1002/smll.201403071
103. Y. Wang, C.-X. Yang, X.-P. Yan, Hydrothermal and biomineralization synthesis of a dual-modal nanoprobe for targeted near-infrared persistent luminescence and magnetic resonance imaging. Nanoscale **9**(26), 9049–9055 (2017). https://doi.org/10.1039/C7NR02038D
104. Y.-C. Lu, C.-X. Yang, X.-P. Yan, Radiopaque tantalum oxide coated persistent luminescent nanoparticles as multimodal probes for in vivo near-infrared luminescence and computed tomography bioimaging. Nanoscale **7**(42), 17929–17937 (2015). https://doi.org/10.1039/C5NR05623C
105. L.-J. Chen, S.-K. Sun, Y. Wang, C.-X. Yang, S.-Q. Wu, X.-P. Yan, Activatable multifunctional persistent luminescence nanoparticle/copper sulfide nanoprobe for in vivo luminescence imaging-guided photothermal therapy. ACS Appl. Mater. Interfaces **8**(48), 32667–32674 (2016). https://doi.org/10.1021/acsami.6b10702
106. J.-M. Liu, Y.-Y. Liu, D.-D. Zhang, G. Fang, S. Wang Synthesis of plasmon-enhanced near-infrared persistent luminescence $GdAlO_3$:Mn^{4+}, Ge^{4+}@Au core-shell nanoprobes for in vivo tri-modality bioimaging. ACS Appl. Mater. Interfaces **8**(44), 29939–29949 (2016). https://doi.org/10.1021/acsami.6b09580
107. T. Ai, W. Shang, H. Yan, C. Zeng, K. Wang, Y. Gao, T. Guan, C. Fang, J. Tian, Near infrared-emitting persistent luminescent nanoparticles for hepatocellular carcinoma imaging and luminescence-guided surgery. Biomaterials **167**, 216–225 (2018). https://doi.org/10.1016/j.biomaterials.2018.01.031
108. X. Qiu, X. Zhu, M. Xu, Y W. uan, W. Feng, F. Li, Hybrid nanoclusters for near-infrared to near-infrared upconverted persistent luminescence bioimaging. ACS Appl. Mater. Interfaces **9**(38), 32583–32590 (2017). https://doi.org/10.1021/acsami.7b10618
109. S. Carlson, J. Hölsä, T. Laamanen, M. Lastusaari, M. Malkamäki, J. Niittykoski, R. Valtonen, X-ray absorption study of rare earth ions in $Sr_2MgSi_2O_7$:Eu^{2+}, R^{3+} persistent luminescence materials. Opt. Mater. **31**(12), 1877–1879 (2009). https://doi.org/10.1016/j.optmat.2008.12.020
110. S.K. Sharma, A. Bessière, N. Basavaraju, K.R. Priolkar, L. Binet, B. Viana, D. Gourier, Interplay between chromium content and lattice disorder on persistent luminescence of $ZnGa_2O_4$:Cr^{3+} for in vivo imaging. J. Lumin. **155**, 251–256 (2014). https://doi.org/10.1016/j.jlumin.2014.06.056
111. L. Ma, X. Zou, B. Bui, W. Chen, K. Song, T. Solberg, X-ray excited ZnS:Cu, Co afterglow nanoparticles for photodynamic activation. Appl. Phys. Lett. **105**(1), 13702 (2014). https://doi.org/10.1063/1.4890105
112. K. Santacruz-Gomez, R. Meléndrez, M.I. Gil-Tolano, J.A. Jimenez, M.T. Makale et al., Thermally stimulated luminescence and persistent luminescence of β-irradiated YAG:Pr^{3+} nanophosphors produced by combustion synthesis. Radiat. Meas. **94**, 35–40 (2016). https://doi.org/10.1016/j.radmeas.2016.09.001
113. X. Li, Z. Xue, M. Jiang, Y. Li, S. Zeng, H. Liu, Soft X-ray activated $NaYF_4$:Gd/Tb scintillating nanorods for in vivo dual-modal X-ray/X-ray-induced optical bioimaging. Nanoscale **10**(1), 342–350 (2017). https://doi.org/10.1039/c7nr02926h
114. Z. Xue, X. Li, Y. Li, M. Jiang, H. Liu, S. Zeng, J. Hao, X-ray-activated near-infrared persistent luminescent probe for deep-tissue and renewable in vivo bioimaging. ACS Appl. Mater. Interfaces **9**(27), 22132–22142 (2017). https://doi.org/10.1021/acsami.7b03802
115. L. Song, X.-H. Lin, X.-R. Song, S. Chen, X.-F. Chen, J. Li, H.-H. Yang, Repeatable deep-tissue activation of persistent luminescent nanoparticles by soft X-ray for high sensitivity

long-term in vivo bioimaging. Nanoscale **9**(8), 2718–2722 (2017). https://doi.org/10.1039/C6NR09553D

116. E. Rodríguez, G. López-Peña, E. Montes, G. Lifante, J. Solé, D. Jaque, L. Diaz-Torres, P. Salas, Persistent luminescence nanothermometers. Appl. Phys. Lett. **111**(8), 81901 (2017). https://doi.org/10.1063/1.4990873
117. J. Xu, D. Murata, Y. Katayama, J. Ueda, S. Tanabe, Cr^{3+}/Er^{3+} co-doped $LaAlO_3$ perovskite phosphor: a near-infrared persistent luminescence probe covering the first and third biological windows. J. Mater. Chem. B **5**(31), 6385–6393 (2017). https://doi.org/10.1039/C7TB01332A
118. J. Shi, X. Sun, S. Zheng, J. Li, X. Fu, H. Zhang, A new near-infrared persistent luminescence nanoparticle as a multifunctional nanoplatform for multimodal imaging and cancer therapy. Biomaterials **152**, 15–23 (2018). https://doi.org/10.1016/j.biomaterials.2017.10.032
119. S. Kamimura, X.U. Chao-Nan, H. Yamada, G. Marriott, K. Hyodo, T. Ohno, Near-infrared luminescence from double-perovskite $Sr_3Sn_2O_7$:Nd^{3+}: a new class of probe for in vivo imaging in the second optical window of biological tissue. J. Ceram. Soc. Jpn. **125**(7), 591–595 (2017). https://doi.org/10.2109/jcersj2.17051
120. L. Zhou, T. Qiu, F. Lv, L. Liu, J. Ying, S. Wang, Self-assembled nanomedicines for anticancer and antibacterial applications. Adv. Healthc. Mater. **7**(20), e1800670 (2018). https://doi.org/10.1002/adhm.201800670
121. T. Maldiney, B. Ballet, M. Bessodes, D. Scherman, C. Richard Mesoporous persistent nanophosphors for in vivo optical bioimaging and drug-delivery. Nanoscale 6(22), 13970–13976 (2014). https://doi.org/10.1039/C4NR03843F
122. L.-J. Chen, C.-X. Yang, X.-P. Yan, Liposome-coated persistent luminescence nanoparticles as luminescence trackable drug carrier for chemotherapy. Anal. Chem. **89**(13), 6936–6939 (2017). https://doi.org/10.1021/acs.analchem.7b01397
123. H.J. Zhang, X. Zhao, L.J. Chen, C.X. Yang, X.P. Yan, pH-driven targeting nanoprobe with dual-responsive drug release for persistent luminescence imaging and chemotherapy of tumor. Anal. Chem. **92**(1), 1179–1188 (2020). https://doi.org/10.1021/acs.analchem.9b04318
124. Y. Feng, R. Liu, L. Zhang, Z. Li, Y. Su, Y. Lv Raspberry-like mesoporous $Zn_{1.07}Ga_{2.34}Si_{0.98}O_{6.56}$:$Cr_{0.01}$ nanocarriers for enhanced near-infrared afterglow imaging and combined cancer chemotherapy. ACS Appl. Mater. Interfaces 11(48), 44978–44988 (2019). https://doi.org/10.1021/acsami.9b18124
125. Y. Lv, D. Ding, Y. Zhuang, Y. Feng, J. Shi, H. Zhang, T.L. Zhou, H. Chen, R.J. Xie, Chromium-doped zinc gallogermanate@zeolitic imidazolate framework-8: a multifunctional nanoplatform for rechargeable in vivo persistent luminescence imaging and pH-responsive drug release. ACS Appl. Mater. Interfaces **11**(2), 1907–1916 (2019). https://doi.org/10.1021/acsami.8b19172
126. H. Zhao, G. Shu, J. Zhu, Y. Fu, Z. Gu, D. Yang, Persistent luminescent metal–organic frameworks with long-lasting near infrared emission for tumor site activated imaging and drug delivery. Biomaterials **217**, 119332 (2019). https://doi.org/10.1016/j.biomaterials.2019.119332
127. W. Jiang, L. Huang, F. Mo, Y. Zhong, L. Xu, F. Fu, Persistent luminescent multifunctional drug delivery nano-platform based on nanomaterial $ZnGa_2O_4$:Cr^{3+}, Sn^{4+} for imaging-guided cancer chemotherapy. J. Mater. Chem. B **7**(18), 3019–3026 (2019). https://doi.org/10.1039/c9tb00109c
128. G. Liu, S. Zhang, Y. Shi, X. Huang, Y. Tang, P. Chen, W. Si, W. Huang, X. Dong, "Wax-sealed" theranostic nanoplatform for enhanced afterglow imaging-guided photothermally triggered photodynamic therapy. Adv. Funct. Mater. **28**(42), 1804317 (2018). https://doi.org/10.1002/adfm.201804317
129. L. Hu, P. Wang, M. Zhao, L. Liu, L. Zhou et al., Near-infrared rechargeable "optical battery" implant for irradiation-free photodynamic therapy. Biomaterials **163**, 154–162 (2018). https://doi.org/10.1016/j.biomaterials.2018.02.029
130. S.K. Sun, J.C. Wu, H. Wang, L. Zhou, C. Zhang, R. Cheng, D. Kan, X. Zhang, C. Yu, Turning solid into gel for high-efficient persistent luminescence-sensitized photodynamic therapy. Biomaterials **218**, 119328 (2019). https://doi.org/10.1016/j.biomaterials.2019.119328
131. R. Abdurahman, C.-X. Yang, X.-P. Yan, Conjugation of a photosensitizer to near infrared light renewable persistent luminescence nanoparticles for photodynamic therapy. Chem. Commun. **52**(90), 13303–13306 (2016). https://doi.org/10.1039/C6CC07616E
132. J. Wang, Y. Li, R. Mao, Y. Wang, X. Yan, J. Liu, Persistent luminescent nanoparticles as energy mediators for enhanced photodynamic therapy with fractionated irradiation. J. Mater. Chem. B **5**(29), 5793–5805 (2017). https://doi.org/10.1039/C7TB00950J
133. T. Ozdemir, Y.C. Lu, S. Kolemen, E. Tanriverdi-Ecik, E.U. Akkaya, Generation of singlet oxygen by persistent luminescent nanoparticle–photosensitizer conjugates: a proof of principle for photodynamic therapy without light. Chem. Photo. Chem. **1**(5), 183–187 (2017). https://doi.org/10.1002/cptc.201600049
134. W. Fan, N. Lu, C. Xu, Y. Liu, J. Lin et al., Enhanced afterglow performance of persistent luminescence implants for efficient repeatable photodynamic therapy. ACS Nano **11**, 5864–5872 (2017). https://doi.org/10.1021/acsnano.7b01505
135. B. Zheng, H.-B. Chen, P.-Q. Zhao, H.-Z. Pan, X.-L. Wu, X.-Q. Gong, H.-J. Wang, J. Chang, Persistent luminescent nanocarrier as an accurate tracker in vivo for near infrared-remote selectively triggered photothermal therapy. ACS Appl. Mater. Interfaces **8**(33), 21603–21611 (2016). https://doi.org/10.1021/acsami.6b07642
136. P. Zhao, W. Ji, S. Zhou, L. Qiu, L. Li, Z. Qian, X. Liu, H. Zhang, X. Cao, Upconverting and persistent luminescent nanocarriers for accurately imaging-guided photothermal therapy. Mat. Sci. Eng. C **79**, 191–198 (2017). https://doi.org/10.1016/j.msec.2017.05.046
137. H. Chen, B. Zheng, C. Liang, L. Zhao, Y. Zhang et al., Near-infrared persistent luminescence phosphors $ZnGa_2O_4$:Cr^{3+} as an accurately tracker to photothermal therapy in vivo

 https://doi.org/10.1007/s40820-020-0404-8

for visual treatment. Mat. Sci. Eng. C **79**, 372–381 (2017). https://doi.org/10.1016/j.msec.2017.05.053

138. S.Q. Wu, C.X. Yang, X.P. Yan, A dual-functional persistently luminescent nanocomposite enables engineering of mesenchymal stem cells for homing and gene therapy of glioblastoma. Adv. Funct. Mater. **27**(11), 1604992 (2017). https://doi.org/10.1002/adfm.201604992
139. L. Qin, P. Yan, C. Xie, J. Huang, Z. Ren, X. Li, S. Best, X. Cai, G. Han, Gold nanorod-assembled $ZnGa_2O_4$:Cr nanofibers for led-amplified gene silencing in cancer cells. Nanoscale **10**(28), 13432–13442 (2018). https://doi.org/10.1039/c8nr03802c
140. Y. Zhang, F. Wang, E. Ju, Z. Liu, Z. Chen, J. Ren, X. Qu, Metal-organic-framework-based vaccine platforms for enhanced systemic immune and memory response. Adv. Funct. Mater. **26**(35), 6454–6461 (2016). https://doi.org/10.1002/adfm.201600650
141. M.H. Spitzer, Y. Carmi, N.E. Reticker-Flynn, S.S. Kwek, D. Madhireddy et al., Systemic immunity is required for effective cancer immunotherapy. Cell **168**(3), 487–490 (2017). https://doi.org/10.1016/j.cell.2016.12.022
142. T. Maldiney, C. Richard, J. Seguin, N. Wattier, M. Bessodes, D. Scherman, Effect of core diameter, surface coating, and peg chain length on the biodistribution of persistent luminescence nanoparticles in mice. ACS Nano **5**(2), 854–862 (2011). https://doi.org/10.1021/nn101937h
143. T. Maldiney, G. Byk, N. Wattier, J. Seguin, R. Khandadash, M. Bessodes, C. Richard, D. Scherman, Synthesis and functionalization of persistent luminescence nanoparticles with small molecules and evaluation of their targeting ability. Int. J. Pharmaceut. **423**(1), 102–107 (2012). https://doi.org/10.1016/j.ijpharm.2011.06.048
144. T. Maldiney, M. Rémond, M. Bessodes, D. Scherman, C. Richard, Controlling aminosilane layer thickness to extend the plasma half-life of stealth persistent luminescence nanoparticles in vivo. J. Mater. Chem. B **3**(19), 4009–4016 (2015). https://doi.org/10.1039/C5TB00146C
145. G. Ramírez-García, S. Gutiérrez-Granados, M.A. Gallegos-Corona, L. Palma-Tirado, F. d'Orlyé et al., Long-term toxicological effects of persistent luminescence nanoparticles after intravenous injection in mice. Int. J. Pharmaceut. **532**(2), 686–695 (2017). https://doi.org/10.1016/j.ijpharm.2017.07.015
146. Y. Jiang, Y. Li, C. Richard, D. Scherman, Y. Liu, Hemocompatibility investigation and improvement of near-infrared persistent luminescent nanoparticle $ZnGa_2O_4$:Cr^{3+} by surface pegylation. J. Mater. Chem. B **7**(24), 3796–3803 (2019). https://doi.org/10.1039/c9tb00378a
147. L. Wang, J. Zhang, B. Qu, Q. Wu, R. Zhou et al., Mechanistic insights into tunable luminescence and persistent luminescence of the full-color-emitting bcno phosphors. Carbon **122**, 176–184 (2017). https://doi.org/10.1016/j.carbon.2017.06.054
148. X. Yang, D. Yan, Strongly enhanced long-lived persistent room temperature phosphorescence based on the formation of metal–organic hybrids. Adv. Opt. Mater. **4**(6), 897–905 (2016). https://doi.org/10.1002/adom.201500666
149. X. Yang, D. Yan, Long-afterglow metal–organic frameworks: reversible guest-induced phosphorescence tunability. Chem. Sci. **7**(7), 4519–4526 (2016). https://doi.org/10.1039/C6SC00563B
150. J. Liu, Y. Zhuang, L. Wang, T. Zhou, N. Hirosaki, R.J. Xie, Achieving multicolor long-lived luminescence in dye-encapsulated metal–organic frameworks and its application to anticounterfeiting stamps. ACS Appl. Mater. Interfaces **10**(2), 1802–1809 (2018). https://doi.org/10.1021/acsami.7b13486
151. Z. Wang, C.Y. Zhu, S.Y. Yin, Z.W. Wei, J.H. Zhang, Y.N. Fan, J.J. Jiang, M. Pan, C.Y. Su, A metal–organic supramolecular box as a universal reservoir of UV, WL, and NIR light for long-persistent luminescence. Angew. Chem. Int. Ed. **58**(11), 3481–3485 (2019). https://doi.org/10.1002/anie.201812708
152. Z. Cheng, H. Shi, H. Ma, L. Bian, Q. Wu et al., Ultralong phosphorescence from organic ionic crystals under ambient conditions. Angew. Chem. Int. Ed. **57**(3), 678–682 (2018). https://doi.org/10.1002/anie.201710017
153. J. Han, W. Feng, D.Y. Muleta, C.N. Bridgmohan, Y. Dang et al., Small-molecule-doped organic crystals with long-persistent luminescence. Adv. Funct. Mater. **29**(30), 1902503 (2019). https://doi.org/10.1002/adfm.201902503
154. B. Zhou, D. Yan, Simultaneous long-persistent blue luminescence and high quantum yield within 2D organic-metal halide perovskite micro/nanosheets. Angew. Chem. Int. Ed. **58**(42), 15128–15135 (2019). https://doi.org/10.1002/anie.201909760
155. P. Xue, P. Wang, P. Chen, B. Yao, P. Gong, J. Sun, Z. Zhang, R. Lu, Bright persistent luminescence from pure organic molecules through a moderate intermolecular heavy atom effect. Chem. Sci. **8**(9), 6060–6065 (2015). https://doi.org/10.1039/C5SC03739E
156. M. Palner, K. Pu, S. Shao, J. Rao, Semiconducting polymer nanoparticles with persistent near-infrared luminescence for in vivo optical imaging. Angew. Chem. Int. Ed. **127**(39), 11639–11642 (2015). https://doi.org/10.1002/ange.201502736
157. X. Zhen, Y. Tao, Z. An, P. Chen, C. Xu, R. Chen, W. Huang, K. Pu, Ultralong phosphorescence of water-soluble organic nanoparticles for in vivo afterglow imaging. Adv. Mater. **29**(33), 1606665 (2017). https://doi.org/10.1002/adma.201606665
158. J. Li, J. Rao, K. Pu, Recent progress on semiconducting polymer nanoparticles for molecular imaging and cancer phototherapy. Biomaterials **155**, 217–235 (2018). https://doi.org/10.1016/j.biomaterials.2017.11.025
159. Y. Lyu, X. Zhen, Y. Miao, K. Pu, Reaction-based semiconducting polymer nanoprobes for photoacoustic imaging of protein sulfenic acids. ACS Nano **11**(1), 358–367 (2017). https://doi.org/10.1021/acsnano.6b05949
160. Y. Lyu, D. Cui, H. Sun, Y. Miao, H. Duan, K. Pu, Dendronized semiconducting polymer as photothermal

nanocarrier for remote activation of gene expression. Angew. Chem. Int. Ed. **56**(31), 9155–9159 (2017). https://doi.org/10.1002/anie.201705543

161. C. Xie, X. Zhen, Q. Miao, Y. Lyu, K. Pu, Self-assembled semiconducting polymer nanoparticles for ultrasensitive near-infrared afterglow imaging of metastatic tumors. Adv. Mater. **30**(21), e1801331 (2018). https://doi.org/10.1002/adma.201801331
162. J. Li, Z. Hai, H. Xiao, X. Yi, G. Liang, Intracellular self-assembly of $Ru(bpy)_3^{2+}$ nanoparticles enables persistent phosphorescence imaging of tumors. Chem. Commun. **54**(28), 3460–3463 (2018). https://doi.org/10.1039/C8CC01759J
163. S. He, C. Xie, Y. Jiang, K. Pu, An organic afterglow protheranostic nanoassembly. Adv. Mater. **31**(32), e1902672 (2019). https://doi.org/10.1002/adma.201902672
164. X. Ni, X. Zhang, X. Duan, H.L. Zheng, X.S. Xue, D. Ding, Near-infrared afterglow luminescent aggregation-induced emission dots with ultrahigh tumor-to-liver signal ratio for promoted image-guided cancer surgery. Nano Lett. **19**(1), 318–330 (2019). https://doi.org/10.1021/acs.nanolett.8b03936
165. T. Lecuyer, M.A. Durand, J. Volatron, M. Desmau, R. Lai-Kuen, Y. Corvis et al., Degradation of $ZnGa_2O_4:Cr^{3+}$ luminescent nanoparticles in lysosomal-like medium. Nanoscale (2020). https://doi.org/10.1039/c9nr06867h
166. J. Wang, Q. Ma, W. Zheng, H. Liu, C. Yin, F. Wang, X. Chen, Q. Yuan, W. Tan, One-dimensional luminous nanorods featuring tunable persistent luminescence for autofluorescence-free biosensing. ACS Nano **11**(8), 8185–8191 (2017). https://doi.org/10.1021/acsnano.7b03128
167. R.H. Wang, C.L. Zhu, L.L. Wang, L.Z. Xu, W.L. Wang, C. Yang, Y. Zhang, Dual-modal aptasensor for the detection of isocarbophos in vegetables. Talanta **205**, 120094 (2019). https://doi.org/10.1016/j.talanta.2019.06.094
168. F. Feng, X. Chen, G. Li, S. Liang, Z. Hong, H.F. Wang, Afterglow resonance energy transfer inhibition for fibroblast activation protein-alpha assay. ACS Sensors **3**(9), 1846–1854 (2018). https://doi.org/10.1021/acssensors.8b00680
169. J. Li, C. Yang, W.L. Wang, X.P. Yan, Functionalized gold and persistent luminescence nanoparticle-based ratiometric absorption and TR-FRET nanoplatform for high-throughput sequential detection of L-cysteine and insulin. Nanoscale **10**(31), 14931–14937 (2018). https://doi.org/10.1039/c8nr04414g
170. Y. Liu, Y. Wang, K. Jiang, S. Sun, S. Qian, Q. Wu, H. Lin, A persistent luminescence-based label-free probe for the ultrasensitive detection of hemoglobin in human serum. Talanta **206**, 120206 (2020). https://doi.org/10.1016/j.talanta.2019.120206
171. X. Zhang, N.-Y. Xu, Q. Ruan, D.-Q. Lu, Y.-H. Yang, R. Hu, A label-free and sensitive photoluminescence sensing platform based on long persistent luminescence nanoparticles for the determination of antibiotics and 2,4,6-trinitrophenol. RSC Adv. **8**(11), 5714–5720 (2018). https://doi.org/10.1039/c7ra12222e
172. K. Ge, J. Liu, P. Wang, G. Fang, D. Zhang, S. Wang, Near-infrared-emitting persistent luminescent nanoparticles modified with gold nanorods as multifunctional probes for detection of arsenic(III). Microchim. Acta **186**(3), 197 (2019). https://doi.org/10.1007/s00604-019-3294-z

 https://doi.org/10.1007/s40820-020-0404-8